Journal of Water Process Engineering 70 (2025) 106919

Contents lists available at ScienceDirect

Journal of Water Process Engineering

journal homepage: www.elsevier.com/locate/jwpe

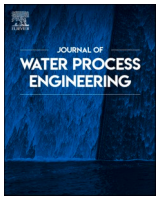

Optimizing anaerobic digestion of palm oil mill effluent (POME) with biochar: Synergistic impact of biochar addition and kinetic analysis

Shaet Jing Yan [a], Yi Jing Chan [a,*], Suchithra Thangalazhy-Gopakumar [a], Timm Joyce Tiong [a], Jun Wei Lim [b]

[a] Department of Chemical and Environmental Engineering, University of Nottingham Malaysia, Broga Road, 43500 Semenyih, Selangor, Malaysia
[b] HICoE-Centre for Biofuel and Biochemical Research, Institute of Sustainable Energy and Resources, Department of Fundamental and Applied Sciences, Universiti Teknologi PETRONAS, 32610 Seri Iskandar, Perak Darul Ridzuan, Malaysia

ARTICLE INFO

Editor: H.H. NGO

Keywords:
Anaerobic digestion
Palm oil mill effluent
Biochar
Kinetic analysis
Optimization

ABSTRACT

This study investigates the synergistic potential of biochar to improve Palm Oil Mill Effluent (POME) treatment through anaerobic digestion (AD) under mesophilic conditions, focusing on the effects of biochar dosage (0.5 to 2.0 g), feed-to-inoculum (FI) ratio (0.16 to 1.00), and organic loading (OL) (1.20 to 5.45 g VS/L) on AD performance. The synergistic addition of biochar significantly enhanced the conversion of organic matter into biogas, resulting in 45.0 % higher biogas production, 73.3 % greater methane yield, and a 98.2 % increase in VS removal compared to POME mono-digestion. A Central Composite Design (CCD) within the Response Surface Methodology (RSM) framework was used optimize the process conditions to ensure effective biodegradation and high methane yield with the lowest biochar dosage. The optimal conditions included a low biochar dosage of 0.5 g (equivalent to 2 g/L of reactor volume), a low FI ratio of 0.266, and a high OL of 4.536 g VS/L. These conditions were validated in duplicate, resulting in 2950 mL of biogas, with a methane yield of 0.355 L/g VS and a VS removal of 95.1 %. The Transference Function Model (TFM) was identified as the most accurate kinetic model for predicting methane yield, demonstrating minimal error.

1. Introduction

In 2023, the global palm oil consumption is found to be around 77 million tonnes, highlighting the crucial role of palm oil mill to meet this growing demand [1]. Palm oil mill plays a vital role in extracting palm oil and palm kernel oil from fresh fruit bunches (FFB), with a notably focus on oil recovery technologies to minimize profit loss and environmental impacts [2]. In general, the palm oil milling process can be categorised into a dry and a wet (standard) process, with the wet process being the most common method employed in Malaysia. In the wet process, palm oil is extracted using hot water leaching, resulting in significant water consumption [3]. Literatures have indicated that producing a ton of crude palm oil requires Kamyab 5–7.5 t of water, with over 50 % of this water ends up as palm oil mill effluent (POME) [4].

Raw POME from palm oil mills is a complex mixture, comprising water, residual oil, organic materials and total solid (TS) [5]. The oil and organic compounds present in POME results in elevated levels of biochemical oxygen demand (BOD) and chemical oxygen demand (COD), hindering natural decomposition processes [6]. Large amount of organic nitrogen, potassium and phosphorus present in POME also promotes algae growth [7]. POME is non-toxic, however discharging of untreated POME into rivers, streams or lakes leads to aquatic ecosystem contamination, causing acidification and eutrophication of water bodies [8]. Consequently, raw POME is recognized as one of the most harmful wastes if left untreated at the mill [80]. Therefore, effective treatment processes are essential to ensure that POME meets the department of environment (DOE) standards, as shown in Table A1.

In recent years, many attempts, such as physical treatment, chemical treatment, aerobic digestion, anaerobic digestion (AD), anaerobic ponding system and membrane anaerobic system have been explored for POME treatment [9,10]. Each of these treatment methods offers unique advantages and challenges in addressing the complex composition of POME and its environmental impacts. Among these approaches, AD stands out for its energy savings, methane production, minimal nutrient requirements and efficient sludge management [5]. AD not only facilitates the degradation of organic pollutants in POME but also offers the

* Corresponding author.
E-mail address: Yi-Jing.Chan@nottingham.edu.my (Y.J. Chan).

https://doi.org/10.1016/j.jwpe.2024.106919
Received 24 September 2024; Received in revised form 18 December 2024; Accepted 30 December 2024
Available online 9 January 2025
2214-7144/© 2025 The Authors. Published by Elsevier Ltd. This is an open access article under the CC BY-NC-ND license (http://creativecommons.org/licenses/by-nc-nd/4.0/).

potential for resource recovery through the generation of biogas, contributing to the sustainability of palm oil mill operations and reduction of their environmental footprint [11]. Therefore, AD holds promise as a viable and environmentally friendly treatment option to mitigate the harmful effects of POME for discharge.

AD is a multistage biochemical process, involving conversion of POME into methane, carbon dioxide and water in the absence of oxygen and presence of anaerobic microorganisms. This process is carried out in digesters under mesophilic (35 °C) or thermophilic (55 °C) condition. The efficiency of the AD process is substantially influenced by the metabolic interactions among the distinct microorganisms [12]. Under AD process, the diverse group of microorganisms collaboratively hydrolyses organic matter, converting them into simpler compounds, such as amino acids, fatty acids and sugar [13]. Subsequently, these hydrolysed compounds undergo acetogenesis and methanogenesis, producing biogas. The biogas predominantly consists of methane and carbon dioxide; therefore, biogas holds the potential for energy generation [14].

The AD process can be implemented through various method, such as ponding treatment, anaerobic filtration and up-flow anaerobic sludge blanket (UASB) reactors [5]. In Malaysia, palm oil mills traditionally employ ponding treatment, a cost-effective method where stages of pond retain POME and treat it through anaerobic treatment [15]. Despite its cost efficiency, this method faces challenges in energy recovery, ungoverned emissions of greenhouse gas and lengthy retention time. Consequently, researchers have shifted their focus to anaerobic digestion coupled with systematic biogas capture to ensure sustainable milling practices [16]. The captured biogas serves as an on-site energy source, offering potential cost savings and resource optimization. Biogas capturing has been practiced in palm oil mills for years; however, it is hindered by low methane productivity due to variability in POME characteristics and fluctuations in flow rates [80]. These factors negatively impact overall system performance, leading to inconsistent biogas production. Therefore, there remains a critical need to optimize this AD process for improved stability, enhanced methane production, and mitigation of inhibition issues [17].

Biochar addition in AD has drawn significant attention from researchers and is recognized as an effective method to enhance AD stability and methane production by speeding up the methanogenesis stage [18]. Biochar, a highly porous carbonaceous solid product from pyrolysis, is sourced from various feedstocks such as wood, livestock manure and spent coffee ground [19]. Several studies have highlighted the potential of biochar addition due to its physiochemical properties [20,21]. The high specific surface area and electron donating capacity facilitate the growth of bacteria involved in glucose decomposition, thereby further enhancing methane production in the early stage of AD [22]. Furthermore, biochar has been found to alleviate inhibitory toxins, shorten the methanogenic lag phase, immobilize functional microbes, and expedite electron transfer between methanogenic and acetogenic microbes in the AD process [23]. Zhang et al. [24] demonstrated the effectiveness of biochar addition in AD of sewage sludge, revealing that appropriate addition of biochar improves the methane yield by releasing volatile fatty acid accumulation and alleviating ammonia inhibition.

However, despite the broad application of biochar in AD systems for other wastewater types, no prior studies have investigated the use of biochar in the AD of POME. This gap in research represents the core novelty of this study. POME contains high concentrations of organic matter and suspended solids which can pose challenges in the AD process. These compounds may lead to issues such as substrate inhibition, overloading, scum formation, and reduced microbial activity, all of which can hinder the overall efficiency of biogas production. This study is therefore the first to explore the integration of biochar into the AD of POME, focusing on optimizing biogas production, methane yield, and volatile solids (VS) removal, driven by the dual goals of energy recovery and waste reduction. Additionally, palm oil mills generate significant biomass, including empty fruit bunches (EFB), oil palm mesocarp fiber, oil palm kernel shell, palm trunks, and leaves, which are ideal feedstocks for biochar production [87]. Thus, integrating biochar into POME AD not only enhances biogas production but also supports the zero-waste concept by utilizing palm oil mill biomass for biochar production.

A significant aspect of this study is the investigation of synergistic effects between biochar and AD parameters, aiming to enhance overall performance and efficiency. To achieve this, the study begins with an evaluation of the physicochemical properties of POME to assess its biodegradability. Central Composite Design (CCD) in Response Surface Methodology (RSM) is employed to optimize the process by varying biochar dosage, feed (POME) to inoculum (FI) ratios, and organic loading (OL). The relationships between parameters are examined to further refine the process. The effects of these parameters on VS removal, biogas production, and methane yield are then analyzed. Furthermore, a key aspect of the novelty of this study is the strategic effort to minimize biochar dosage to reduce costs, while simultaneously enhancing biogas production compared to the mono-digestion of POME. This approach ensures that the dual objectives are met in a cost-effective manner, without compromising methane yield or overall system performance. Following this, kinetic studies are conducted to identify the most suitable model for predicting AD performance with biochar addition. This synergistic biochar-enhanced AD potentially offers a sustainable approach to addressing the environmental impacts of POME in palm oil production. It can ensure consistent biogas production, even during low crop seasons when POME is limited, and meet the stringent discharge limits set by the Malaysian Department of Environment (DOE), thereby contributing to resource recovery and environmental sustainability.

2. Materials and methods

2.1. Collection and preparation of raw material

In this experiment, POME and inoculum were collected from a palm oil mill located in Selangor, Malaysia. The POME and inoculum were stored at 4 °C prior to the experiment to avoid biodegradation caused by microbial action.

The raw biochar used in the experiment, shown in Fig. 1(a), was generously provided by a pilot biochar production plant located in Eco-PARK, Hong Kong's pioneering recycling-business park. The raw biochar was ground into a fineness of 0.25–20 mm, facilitated by a cutting mill (Retsch SM100, Germany). Following this, the biochar was immersed in deionized water at room temperature and subjected to stirring at 150 rpm using magnetic stirrer (Cole-Parmer, UK). After 30 min of mixing, the solution was filtered with a vacuum pump (Rocker 300, Taiwan). The residue was dried at 105 °C in an oven (Memmert, Germany) for 24 h. The clean, dried ground biochar, depicted in Fig. 1(b), was subsequently stored in a resealable bag to prevent direct exposure to air and moisture.

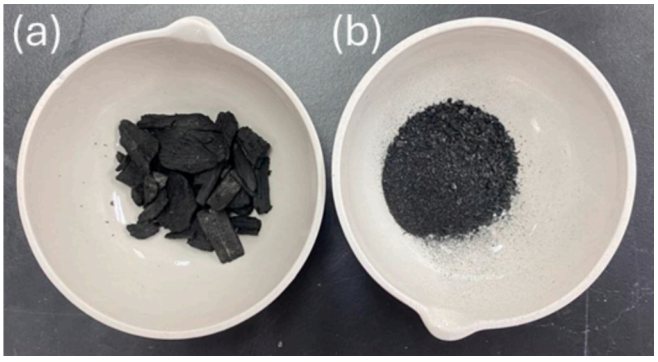

Fig. 1. (a) raw biochar; (b) dried ground biochar.

2.2. Degassing of inoculum

Degassing of inoculum was carried out to ensure the elimination of biogas produced by bacteria in the sludge prior to initiating the AD process of POME. During the process, the anaerobic sludge utilised for the digesters was treated in 250 mL conical flasks and connected to a biogas collection system via graduated fluid bags, with a check valve attached to allow for degassing. The conical flasks were left in a shaker incubator at 125 rpm and 37.5 °C until the biogas production ceased. By removing the methanogenic bioactivity of the microbial inoculum, the degassing process aims to minimize background methane formation in the assays with POME [25].

2.3. Anaerobic digestion system of POME with biochar

The experiment for AD is conducted with three main raw materials: POME, inoculum and biochar. Analysis was performed on the raw materials, mixtures for all experiment sets and the biogas as well as the digestate obtained after the experiment completed, shown in Fig. 2. The characterisation and experiment results were depicted in graphical form, using OriginPro v10.1 software (OriginLab, USA).

For all experiment sets, 250 mL conical flasks were used to accommodate the mixture, consisting of inoculum, POME (substrate) and biochar. The mixture in each set was stirred using a glass rod to ensure properties uniformity. The pH values for all sets were recorded and are close to 7 (neutral). Subsequently, all experiment sets underwent initial characterisation tests, including pH, total solid (TS) and volatile solid (VS). The mixture was then flushed with nitrogen gas for 3–5 min to ensure fully anaerobic conditions. The conical flasks were closed tightly with rubber stopper with a tube connected at the biogas outlet. The tube was then connected to a graduated fluid bag to collect the biogas generated. Parafilm is used to sealed around the stopper to ensure no gas leakage. Fig. 3(a) depicts the experimental setup, an anaerobic digester with biogas collection system.

Consequently, the anaerobic digesters were placed in a shaker incubator, shown in Fig. 3(b), operating at 125 rpm under mesophilic condition. In this study, mesophilic digestion was employed in the experiment. Operating the anaerobic digesters at 37.5 °C delivers enhanced stability performance by fostering a more diverse microbial community, despite producing a lower volume of biogas compared to thermophilic conditions [26]. In palm oil mill, mesophilic processes require less energy input for heating and are generally more resilient to the inhibitory effects of ammonia released during protein mineralization (Z. [27]).

2.4. Analytical methodology

The analytical methodology involved in the initial characterisation of the feed was carried out according to the following sections. The pH of the samples was taken using a portable pH meter probe. Analytical determinations of dissolved oxygen (DO), biological oxygen demand (BOD), chemical oxygen demand (COD), total solids (TS) and VS were carried out in accordance with the Standard Methods for the Examination of Water and Wastewater. The methods, along with the equipment used are stated in Table 1.

2.4.1. Surface morphology analysis

The morphology of biochar, encompassing factors such as particle size, porosity and specific surface area plays a vital role in supporting colonization of microbes and optimizing AD process [28]. Liang et al. [29] highlighted that this property is remarkably influenced by the types of feedstocks and the pyrolysis temperature during biochar production. To gain insights into the raw biochar characteristics and study its surface features after AD process, field emission scanning electron microscopy (FE-SEM) with electron dispersive X-ray (EDX) was conducted. The FE-SEM and EDX analysis in this study utilised the FEI Quanta 400F and Oxford-Instruments INCA 400 with X-Max Detector, respectively.

2.4.2. Biogas and methane yield production

As stated in Section 2.3, the biogas collection system, comprising a graduated fluid bag, was connected to the anaerobic digesters containing the POME, inoculum and biochar mixture. The fluid bag's volume

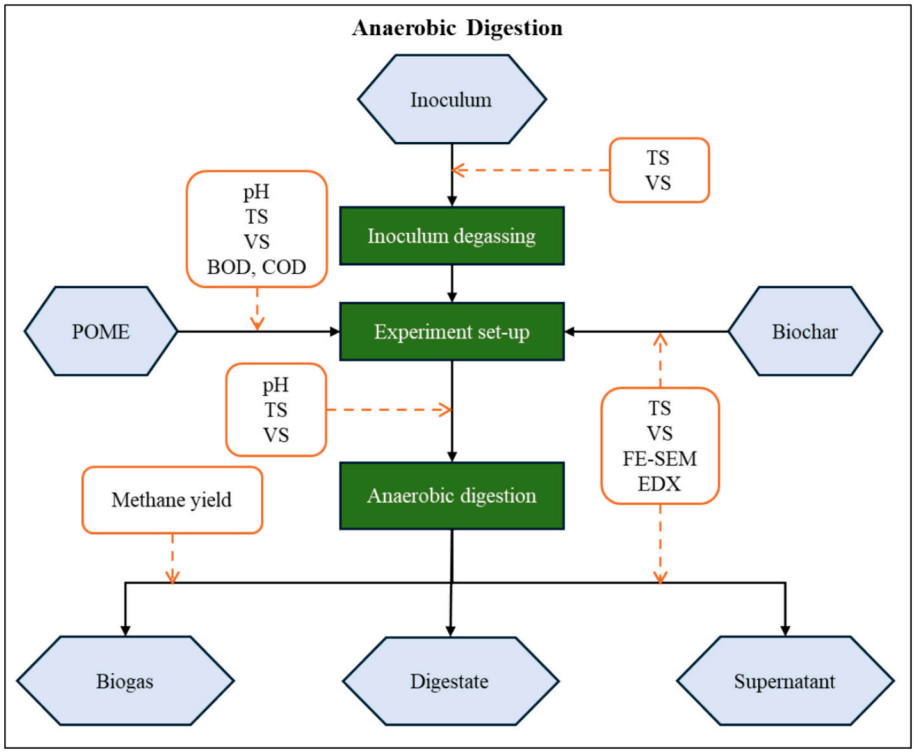

Fig. 2. Experiment flow chart for anaerobic digestion of POME with biochar addition.

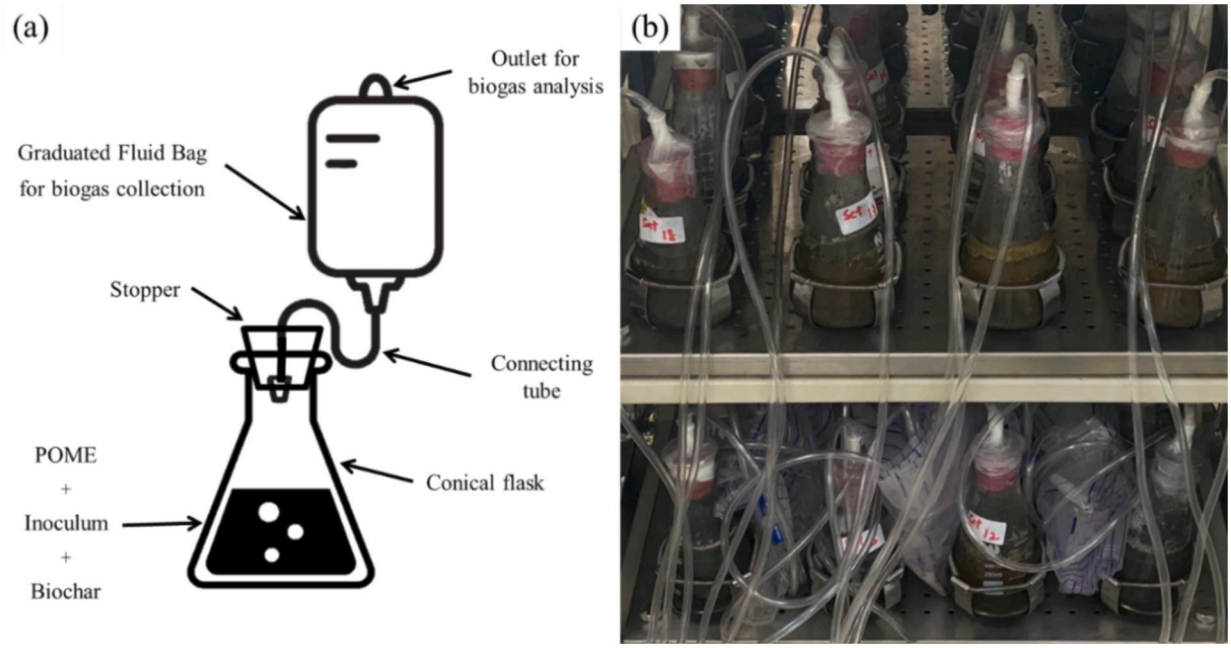

Fig. 3. Experimental set-up and the conical flasks placed in a shaker incubator.

Table 1
Testing methods and their equipment used for analytical measurements.

Test	Methods	Equipment
Biological Oxygen Demand (BOD)	HACH method 8043	YSI 5100 DO meter, USA
Chemical Oxygen Demand (COD)	HACH method 8000	DR2800 Spectrophotometer, USA
Total Solids (TS)	APHA 2540B	Memmert Oven, Germany
Volatile Solids (VS)	APHA 2540E	Nabertherm, Germany

was monitored on every Monday, Wednesday and Friday over a span of 26 days to ensure no gas leakage occurred. This thorough examination ensures that the experiments were conducted with minimal error, resulting in accurate findings. The collected biogas volume was recorded, shown in Table A3. Following the completion of the experiment, the biogas composition for all sets was analysed by using a gas chromatograph (GenTech 7890B, USA) in Universiti Malaya and a biogas analyser (Geotech Biogas 5000, UK). This equipment enabled the testing of methane, carbon dioxide, oxygen and hydrogen sulphide levels within the biogas. The methane yield from the AD process was then calculated with Eq. 1, tabulated in Table A3.

$$Methane\ Yield\ (L/g\ VS) = \frac{Total\ volume\ of\ CH_4(L)}{Mass\ of\ VS\ fed\ (g)} \quad (1)$$

2.5. Experiments design by response surface methodology and central composite design (CCD)

In this study, CCD of RSM was employed to find the optimum conditions for the experiment setup using Design Expert v12 software (Stat-Ease, Inc., USA). RSM utilises optimisation strategies to adjust the settings of factorial variables, aiming to achieve maximum response values [30]. CCD is one of the powerful and crucial tools in modern engineering approach for RSM which provide information exclusively on the effect of experiment variables and overall experimental error with minimal required runs [31]. This approach is commonly adopted by researchers for addressing multi-response problem, considering prior information [32]. Fig. 4 shows the CCD flow diagram for this study.

The factors chosen to be considered in the CCD of RSM for this study are **A**: Biochar dosage, **B**: FI ratio and **C**: OL. Each factor was studied at five levels: centre point, ± 1 and $\pm \alpha$. Constraints were set to eliminate the negative values of variables. The CCD included 20 experiment runs with 3 trials as replication of the central points, resulting in 23 experiments. Table A2 shows the CCD design matrix obtained for the AD system.

The ranges for the experimental factors were determined based on a combination of literature review and preliminary experiments to ensure a comprehensive evaluation of their effects on the AD process.

The FI ratio range of 0.16 and 1.00 was selected to examine its impact on the anaerobic digestion process. Literature indicates that FI ratios below 2 enhance the effectiveness of biochar in AD systems [81,82]. The lower limit of 0.16 represents a scenario where the substrate is in a lower proportion relative to the inoculum, potentially supporting more robust microbial activity due to the abundance of inoculum. The upper limit of 1.00 was chosen to explore the effects of a higher substrate-to-inoculum ratio, where preliminary results still show significant impacts on biogas production and quality.

The biochar dosage range of 0.5–2.5 g was selected to capture its role in enhancing AD performance without introducing adverse effects [88]. Findings from the literature and preliminary experiments suggest that biochar efficacy is dosage-dependent, with lower dosages potentially insufficient for significant improvement and higher dosages risking diminishing returns or instability [18]. The chosen range allows for an optimal balance between enhancing microbial activity and maintaining system stability, enabling thorough investigation of biochar's effect on biogas yield, methane content, and VS removal.

The OL range (1.22–5.45 g VS/L) represents typical operational conditions for AD systems, as reported by Chan et al. [80] and Yusof et al. [86]. The lower limit of 1.22 g VS/L ensures the system operates efficiently under low organic loads, providing insights into biogas production under less stressful conditions. The upper limit of 5.45 g VS/L tests the system's capacity to handle higher organic loads, which is critical for assessing performance under more demanding conditions and for scaling up operations. This range enables a comprehensive analysis of how organic load affects system stability and overall efficiency.

These selected ranges are well-grounded in literature and experimental findings, ensuring that the interactions among these factors are

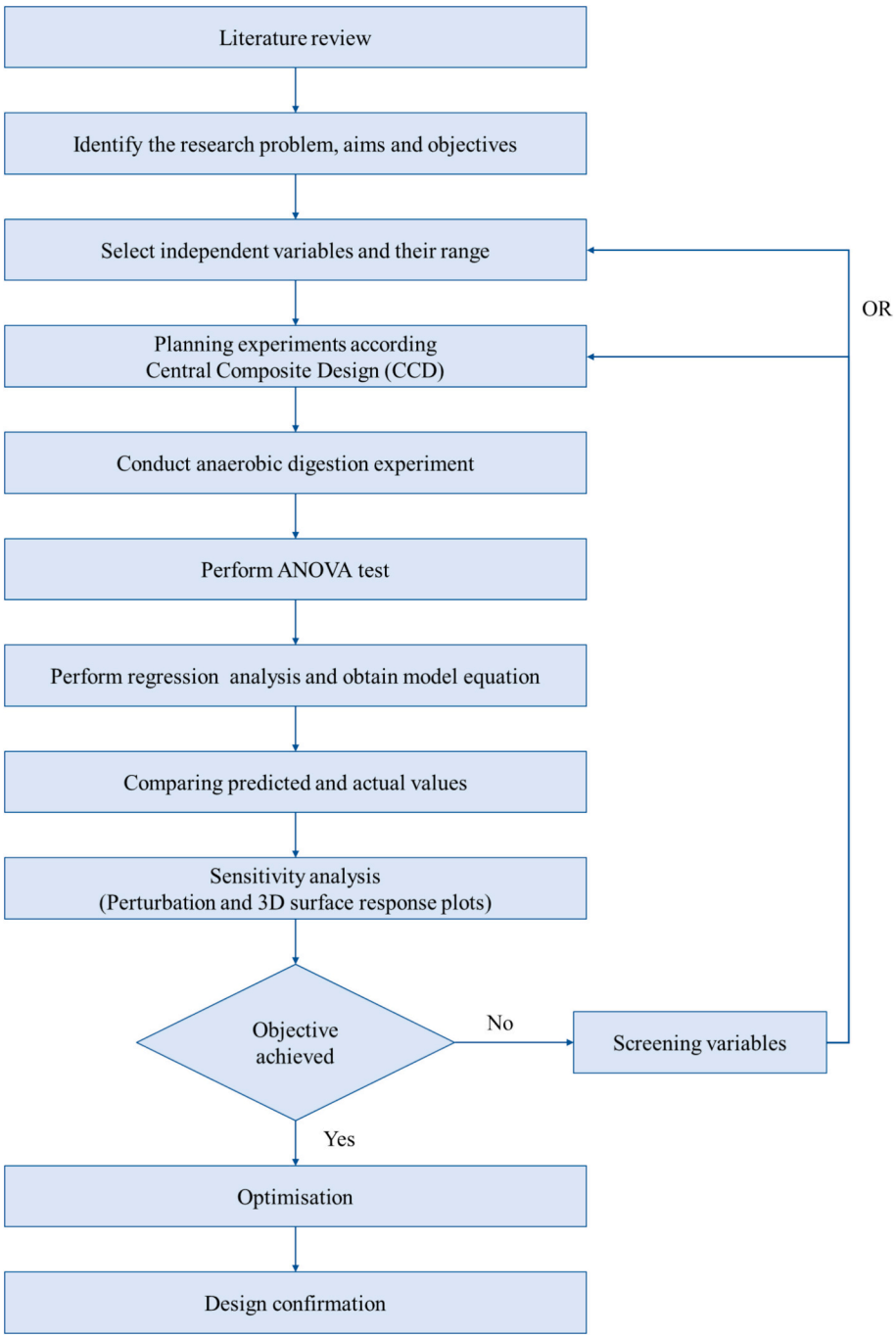

Fig. 4. Methodology flowchart using CCD.

thoroughly investigated for optimizing AD performance.

Three responses, **R1**: Biogas production, **R2**: Methane yield and **R3**: volatile solid (VS) removal, were selected for the system due to their fundamental importance in assessing the performance of the AD system. Biogas production is a key parameter, providing insight into the system's ability to convert organic material into usable energy in the form of biogas. This response helps quantify the overall gas output and is essential for assessing the scalability and economic feasibility of the process. Methane yield, on the other hand, is a more refined measure of efficiency, indicating the proportion of volatile solids (VS) digested that are successfully converted into methane. This metric is particularly important for understanding the energy potential of the biogas produced and how efficiently the process transforms organic waste into a high-energy gas component. Finally, VS removal reflects the degree of organic matter degradation, which is crucial for evaluating the waste treatment effectiveness and stability of the AD process [33]. High VS removal suggests effective digestion, reducing the volume of waste and enhancing the sustainability of the system.

A key innovation of this study lies in the optimization of three variables, biochar dosage, FI ratio, and organic loading, based on all three responses. While most optimization studies focus on a single response or a limited set, this research adopts a more comprehensive approach. By optimizing these variables across biogas production, methane yield, and VS removal, the overall efficiency of the AD system is thoroughly assessed. This comprehensive analysis reflects the dual objectives of the process, which are both energy recovery and waste reduction.

2.6. Statistical analysis and optimisation

Statistical analysis and optimisation were integral components in this study, facilitated by the implementation of CCD for RSM using Design Expert v13 software (Stat-Ease, Inc., USA). The selected model was fitted to the experimental data collected, focusing on the effect of independent variables: (**A**) biochar (g), (**B**) FI ratio and (**C**) OL (g VS/L), on three response variables: (**R1**) VS removal (%), (**R2**) biogas production (mL) and (**R3**) methane yield (g VS/L). The software analysed the experimental data to fit the most suitable model, providing a fit summary for each response.

The process order of the model was selected based on the probability value (*p*-value) from fit summary to produce the analysis of variance (ANOVA) for the selected model. ANOVA is a robust statistical method for analyzing the experimental data and evaluating the fitted model quality. With this approach, the adequacy of the model fit was further verified through coefficient of variation (CV), R^2, adjusted R^2, predicted R^2 and adequate precision. Low CV value indicates high reliability. The adjusted R^2 measures the amount of variation from the mean and the predicted R^2 indicates how well the regression model predict the response for new observation [34]. The difference between R^2 and adjusted R^2 indicates the model adequacy while the difference between adjusted R^2 and predicted R^2 determine the presence of block effect with the data [35].

3D response surface plots were generated through regression analysis of the simulated data, alongside perturbation plots which enabled comparison of the effects of all factors at a specific point in the design space. The response in perturbation plot is generated by varying only one factor over its range while other variables remain constant [35]. The significance of the model terms was assessed using the p-value at a 95 % confidence interval, allowing for the generation of equations in terms of independent variables for response variables. Sensitivity analysis was conducted in the software to identify lower and upper bound for the optimisation parameters. Finally, optimisation of the independent variables was then performed in the software to determine the maximum VS removal, biogas production and methane yield.

2.7. Kinetic studies

There is increasing attention focused on the kinetic characteristics of AD in recent years. Various studies have proposed kinetic model to explain the biogas production with the kinetic parameters. Among mathematical models, Anaerobic Digestion Model No.1 (ADM1) encompasses key chemical pathways, rate equation and inhibition factors, providing accurate predictions with proper calibration ([36]; X. [37]). However, calibration of ADM1 to different AD processes is challenging due to limited knowledge on microbial consortia and complex strain-specific metabolic pathways, requiring extensive analysis [38].

In this study, modified Gompertz model (MGM), logistic function model (LFM) and transference function model (TFM) were adopted to predict the methane gas production and evaluate the anaerobic digestion parameters. MGM is widely used for kinetic study of methane production from AD process. Deepanraj et al. [39] and Matheri et al. [40] have determined that MGM is appropriate for the evaluation of biogas production in their studies. The equation of MGM is shown in Eq. 2. The application of LFM aims to simulate anaerobic fermentation and determine methane production from biodegradation of substrate while TFM, a reaction curve-type model, is applied to anaerobic digestion control processes [41]. Eq. 3 and Eq. 4 show the equations for LFM and TFM respectively.

$$y_{MGM} = A exp\left\{ -exp\left[\frac{\mu_m e}{A}(\lambda - t) + 1\right]\right\} \quad (2)$$

$$y_{LFM} = \frac{A}{1 + exp\left[4\mu_m\left(\frac{\lambda - t}{A}\right) + 2\right]} \quad (3)$$

$$y_{TFM} = A \times \left(1 - exp\left(-\mu_m \times \frac{t - \lambda}{A}\right)\right) \quad (4)$$

where, y is the cumulative methane production (mL/g VS), A is the methane production potential (mL/g VS), μ_m is the maximum methane production (mL/g VS-day), t is time (day), λ is the lag phase (day) and e is a mathematical constant of 2.718282.

2.8. Validation of kinetic studies

To identify the kinetic model that best fits the actual experiment output, the goodness of fit is determined using the root mean square error (RMSE) and coefficient of determination (R^2).

RMSE is commonly used for numerical predictions due to its excellent measure of accuracy [42]. Eq. 5 shows the calculation of RMSE in this report.

$$RMSE = \sqrt{\left(\sum_{i=1}^{n}\frac{(PMY_i - EMY_i)^2}{n}\right)} \quad (5)$$

where, PMY_i is the predicted methane yield, EMY_i is the methane yield obtained from experiment for the ith day of measurement and n is the number of measurements.

R^2, as outlined by Figueiredo et al. [43], is a measure used to evaluate the robustness of relationship between experimental data and values predicted through kinetic studies. The R^2 is determined using Eq. 6.

$$R^2 = 1 - \frac{\sum (EMY_i - PMY_i)^2}{\sum (EMY_i - \overline{EMY})^2} \quad (6)$$

where, PMY_i is the predicted methane yield, EMY_i is the methane yield obtained from experiment for the ith day of measurement and $\overline{EMY}$ is the mean of the experimental methane yield values.

3. Results and discussion

3.1. Characteristics of POME

The comprehensive examination of the POME and inoculum characteristics is crucial for the AD experimental planning. Adjustments such as pH adjustment, FI ratio are performed based on the BOD/COD ratio, VS and initial pH of POME and inoculum. The presented Table 2 reveals the characteristics of POME in this study in comparison with the POME characteristics documented by Lim et al. [44], Prasertsan et al. [46] and Hai et al. [47].

POME characteristics exhibit variability influenced by diverse factors such as the palm fruits quality, processing techniques, crop seasons within the palm oil mill [3]. Hence, slight divergences between the POME analysed in this study and those from prior research studies are anticipated. Notably, Table 2 highlights a dissimilarity in the COD of

Table 2
Comparison of the characteristics of POME with other sources.

Characteristics	Unit	POME in this study	[47]	[46]	[44]
TS	g/L	59.14	32.15	66.20	52.00
VS	g/L	10.91	13.33	44.12	41.89
BOD	g/L	34.99	46.70	–	52.55
COD	g/L	98.77	62.50	88.80	83.42
BOD/COD	–	0.32	0.75	–	0.63
pH	–	4.62	5.5	4.7	4.54

POME, indicating a substantial number of organic pollutants presents within POME. Conversely, the BOD appears relatively lower, while the COD is relatively higher compared to reported values, reflecting the influence of organic compounds and residual oil released during palm oil milling processes [48]. The COD range observed in this study remains within the reported range of 75,000–200,000 mg/L [49], while the BOD range is consistent with the reported range of 10,250–43,750 mg/L [35,50].

The BOD/COD ratio, serving as a key indicator of the POME's biodegradability, has garnered attention from researchers. Previous research has proposed that a BOD/COD ratio exceeding 0.5 suggests high feed biodegradability, rendering it suitable to biological treatment [51]. However, in this investigation, the BOD/COD ratio of POME falls below 0.5, emphasising the necessity to explore the potential effects of biochar addition to improve its biodegradability.

The TS content present in POME falls between the reported values from Prasertsan et al. [46] and Lim et al. [44] as well as the broader range of 11,500–79,000 mg/L reported by Chong et al. [52]. Interestingly, the VS content of POME in this study corresponds closely with value reported by Hai et al. [47], but is comparatively lower compared than those reported by Prasertsan et al. [46] and Lim et al. [44]. Additionally, this VS value is at the lower end of the range of 10,520–31,220 mg/L reported by Trisakti et al. [53]. The initial VS content serves as an energy source for the microorganisms involved biogas production. The addition of biochar into AD system might present a promising avenue to enhance the biogas production, particularly for POME with low VS content. The pH of POME is generally acidic, reflecting the presence of natural fatty acids from palm oil milling [54]. The pH values observed in this study are consistent with those reported in the literature, aligning with the range presented in Table 2 and the findings of Ramón Vanegas et al. [55].

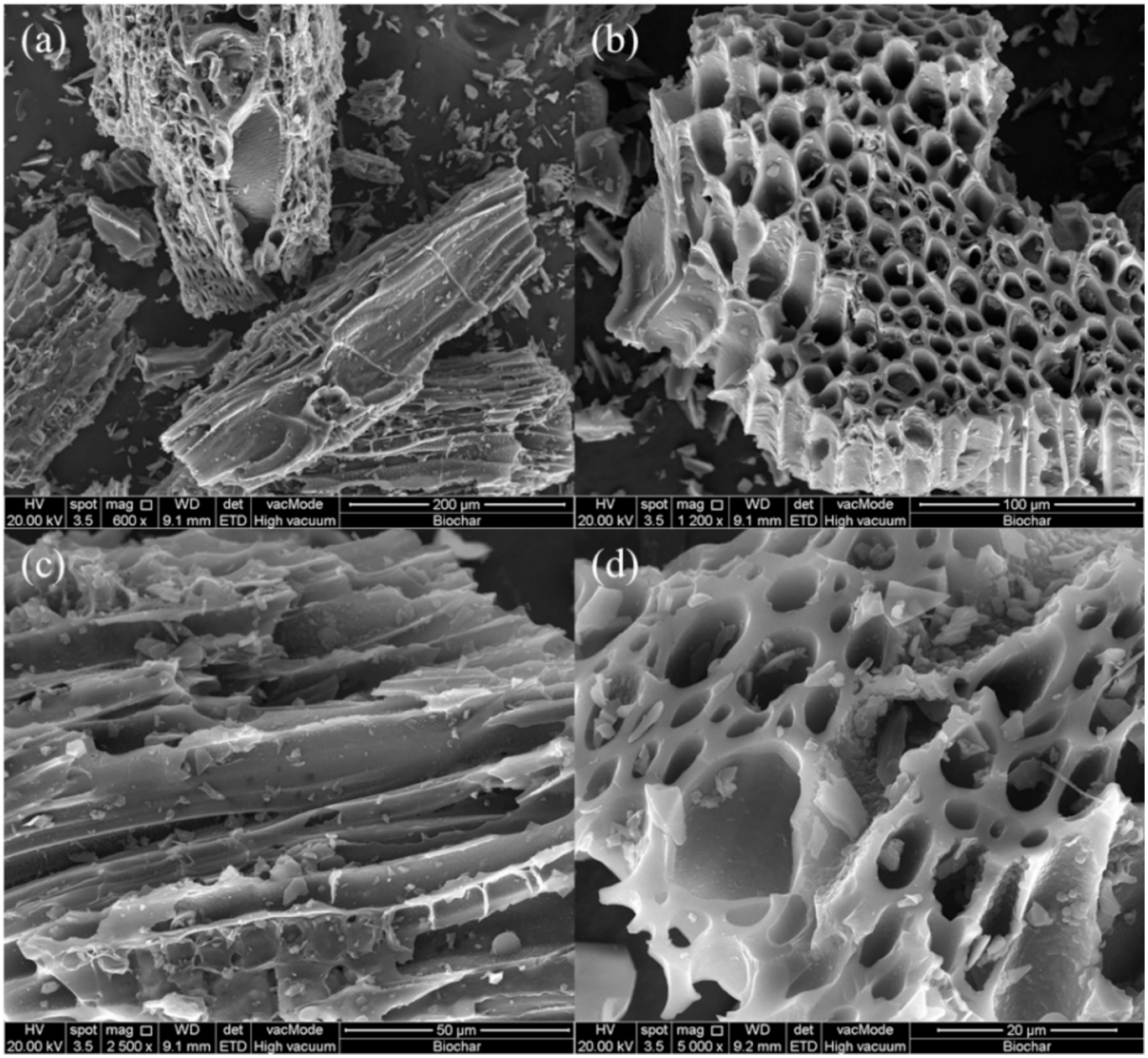

Fig. 5. SEM micrographs of raw biochar magnified by (a) 600 times, (b) 1200 times, (c) 2500 times and (d) 5000 times.

3.2. Morphology analysis of biochar

In this study, wood biomass was used as the raw material for biochar production. The particle size of the biochar ranges from 10 to 500 μm, and its pore size ranges from 2 to 18 μm. This relatively broad particle size distribution allows for flexibility in the biochar's interaction with the surrounding medium, potentially offering both larger surface area for biodegradation and finer particles for enhanced interaction with microorganisms. Fig. 5 illustrates the surface characteristics of the ground, purified biochar after pre-treatment. The biochar exhibits a honeycomb-like porous structure with elongated channels likely formed during high-temperature pyrolysis [56]. W. Zhao et al. [57] have noted that the impact of porosity and specific surface area on the adsorption and immobilization abilities of the biochar. SEM analysis reveals irregular shape pores with size ranging from 5 to 8 μm, evenly distributed on both sides of the channels. Sharp cuts observed on the biochar's sides may be attributed to the grinding process during pre-treatment. The existence of macropores on biochar and the rough surface texture within the channels enhance habitat for microbial growth as well as CO_2 and H_2S removal from biogas [58]. H.-J. Yang et al. [59] reported that the methane production increased by >20 % with addition of biochar, attributed to enhanced CO_2 adsorption.

The electron dispersive X-ray (EDX) analysis results are shown in Fig. 6, with the element weight percentage shown in Table 3. EDX indicates that carbon is the major element present in biochar with small amounts of oxygen, potassium and calcium. Biochar, as a carbon-based material have been shown to enhance methane generation by promoting electron transfer and microbial immobilization (J. [60]). Although avoiding oxygen loading to the AD digestor is crucial, study has shown that limited quantities of oxygen can lead to improved AD performance, hence the small amount of oxygen (7.04 wt%) present in biochar may not cause instability to the AD process [61].

Furthermore, potassium is an element required for microbial growth. While high concentration can cause inhibition or toxicity, small amount of potassium has been shown to positively impact anaerobic microorganism's viability, enhancing AD performance under both thermophilic and mesophilic conditions (Y. [62]; J. [63]). Adequate levels of calcium have been found to support biodegradability and maintain the process stability ([64]; J. [60]). The combined weight percentage of oxygen, potassium and calcium in the biochar is <10 %, mitigating potential negative effects on the AD process while maximizing biogas production efficiency.

3.3. Performance evaluation of biochar addition in anaerobic digestion on methane yield

This study investigates the efficacy of biochar in enhancing overall AD performance through examination and comparison of experimental results with literature findings. The experiment was conducted over a total duration of 26 days, with biogas production ceasing on the final day. This indicates the completion of the anaerobic digestion process

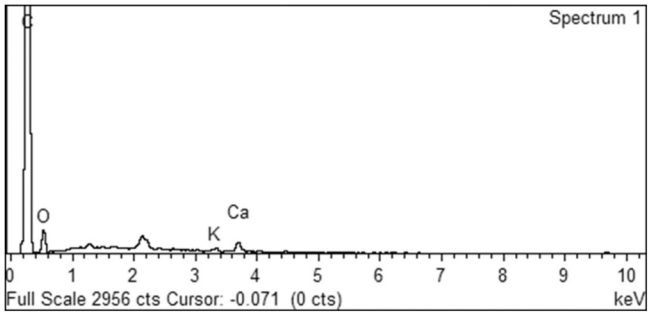

Fig. 6. Electron dispersive X-ray (EDX) of biochar.

Table 3
EDX of the biochar.

Element	Weight Percentage (%)	Atomic Percentage (%)
Carbon	92.33	94.40
Oxygen	7.04	5.40
Potassium	0.15	0.05
Calcium	0.48	0.15

[45]. Fig. 7 depicts the biogas production over time for each set of anaerobic digesters. The cumulative biogas production is found to be gradually increasing, exhibiting a linear upward trend without a lag phase at the beginning of the experiment. This trend aligns with Luo et al. [65], who reported that 10 g/L of biostable biochar addition reduced the lag phase by 38 % in mesophilic anaerobic digesters. Similarly, Kim & Kim [66] found that a substrate-to-inoculum ratio of 0.4–0.6 shortened the lag phase for waste with high protein organic loading. Similar observations were also reported in AD of food waste and biological wastewater, where the addition of biochar shortened the lag phase by 41–54 % [67–69].

In this study, the addition of biochar resulted in significant performance improvements compared to the control, where no biochar was added. Specifically, biogas production, methane yield, and volatile solids (VS) removal were enhanced by 45 %, 73.25 %, and 98.2 %, respectively. These substantial improvements highlight biochar's role not only as a physical support for microbial communities but also as an influential factor in optimizing microbial dynamics. The synergistic effects of biochar addition contribute to enhanced performance metrics, as shown in Fig. 8. These results also align with Shi et al. [70], where adding an optimal dose of biochar (0.60 g/gVS oily sludge) improved CH_4 yield (138.41 mL/gVS) by 119 % compared to the control.

SEM images of biochar post-AD (Fig. 8) offer further insight into the underlying mechanisms driving these improvements. The biochar's surface structure shows decreased porosity and increased roughness, indicating significant microbial attachment and particle accumulation within its pores, consistent with findings by Wang et al. [83]. This microbial colonization suggests that biochar acts as a catalyst, providing a microenvironment that fosters microbial growth and enhances anaerobic digestion efficiency. Furthermore, biochar aids in improving the settling of solids, thus enhancing the removal of VS and improving the digestate's overall quality. Even after the AD process, the biochar retains its porous structure, highlighting its potential for reuse in successive AD cycles and indicating its durability as a microbial support medium.

However, despite these encouraging results, it is essential to critically evaluate the cost-effectiveness of biochar addition. While higher biochar dosages have demonstrated significant benefits in terms of methane yield and VS removal, there is a threshold beyond which additional biochar offers diminishing returns. Excessive biochar may lead to operational challenges, such as clogging or adverse impacts on microbial balance. This highlights the need for a balanced approach where biochar dosage is optimized to achieve maximum performance with minimal input costs. Therefore, further optimization analysis is necessary to fine-tune the synergistic effects of biochar dosage, FI ratio, and OL on biogas production, methane yield, and VS removal. The goal is to strike a balance that maximizes performance while minimizing costs, particularly as biochar can be a costly additive. A trade-off between these factors will be essential for scaling up the process and ensuring its economic feasibility in large-scale applications.

3.4. Response surface methodology (RSM)

3.4.1. Model development and ANOVA analysis

A comprehensive analysis of the effect of **A:** Biochar dosage, **B**: FI ratio and **C**: OL on various aspects of POME AD process is carried out in this section. Key parameters, including **R1**) VS removal (%), (**R2**) biogas production (mL) and (**R3**) methane yield (g VS/L) are thoroughly

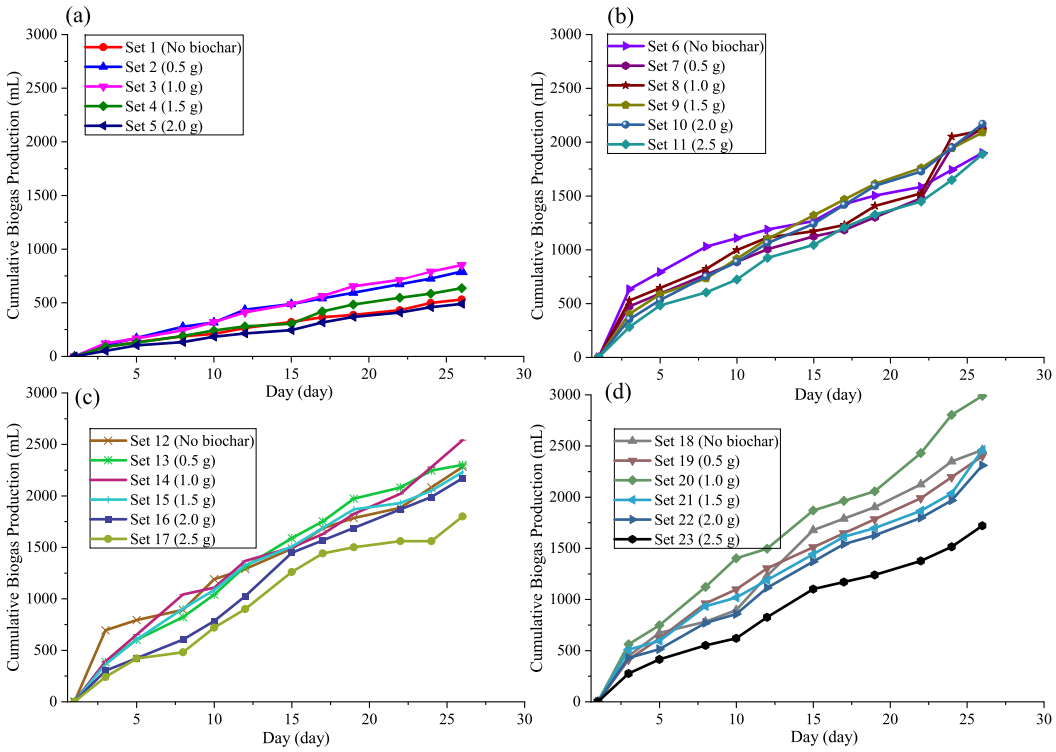

Fig. 7. Cumulative biogas production with FI ratio of (a) 0.16, (b) 0.40, (c) 0.65 and (d) 1.00.

examined. The experimental results are shown in Table A3. Based on the experimental results, ANOVA analysis is carried out to further analyze the significance of the independent variables on the response variables as well as the overall significance of the model. All three response variables show a notable fit to the model. ANOVA analysis for VS removal, biogas production and methane yield are discussed in this section. The fit summaries of the fitted models for all response variables are shown in the Appendix (Table A4).

3.4.1.1. VS removal (R1). For VS removal, the best-fit model is recommended to be the two-factor interaction (2FI) model. The ANOVA results for the model are shown in Table 4. The *p*-value of 0.3116 and the F-value of 1.290 suggest that the 2FI model does not adequately describe the variability in the VS removal data. The individual model terms exhibit *p*-values larger than 0.05, indicating a lack of significant terms for R1. Typically, for a model to be significant, the p-value should be below 0.05, which is not the case here. This indicates that none of the model terms are substantial predictors of VS removal under the given experimental conditions.

Additionally, the 31.16 % probability that the lack-of-fit F-value is due to noise suggests that the observed variability in the data might not be meaningfully captured by this model. This is further reinforced by the negative predicted R^2 value of −0.2021 (Table A4), indicating that even using the overall mean would be more reliable than the 2FI model for predicting VS removal. In simpler terms, the model is ineffective at explaining the trends observed in the data. Moreover, the model's precision value of 3.95, which is below the acceptable threshold, indicates an insufficient signal for navigating the design space. This further confirms the unsuitability of the 2FI model for optimization purposes.

One contributing factor to the model's inadequacy is the narrow range of VS removal observed (from 93 % to 99 %), which limits the model's ability to capture significant effects from the independent variables. The small standard deviation of 3.49 further highlights the lack of variability in the data, which might be due to the high biodegradability of POME, making it difficult to detect meaningful variations in VS removal. This limited variability in the response variable (VS removal) restricts the ability of the model to identify statistically significant effects of biochar dosage, FI ratio, and OL, which are essential for optimization.

While the experimental design and the 2FI model were employed with the intent to optimize VS removal, the results indicate that further exploration of alternative models or adjustments to the experimental setup may be necessary to capture the significant factors influencing VS removal more effectively.

3.4.1.2. Biogas production (R2). The most suitable model for biogas production is the two-factor interaction (2FI) model. The ANOVA results of this model is summarised in Table 5. The overall response model for this response is highly significant with a high F-value (32.40) and low *p*-value (<0.0001), indicating <0.01 % of possibility that noise can cause this huge F-value. From Table 5, it is shown that A (Biochar), C(OL) and BC are significant model terms with a p-value of <0.05.

The model for biogas production has a CV of 12.17 % and a R^2 value of 0.9196, showing that the actual experiment results are close to the predicted response from the model. The predicted R^2 of 0.8218 and the adjusted R^2 of 0.8912 has a difference of <0.2, while the adequate precision of the model is 16.6072. These findings collectively suggest that the 2FI model for biogas production is satisfactory and adequate. The fitted equation for biogas production in terms of the independent variables is generated, shown in Eq. 7.

$$\textit{Biogas Production} = 2292.74 - 211.53 \times A - 254.97 \times B + 835.80 \times C - 405.08 \times AB + 228.37 \times AC - 563.08 \times BC \quad (7)$$

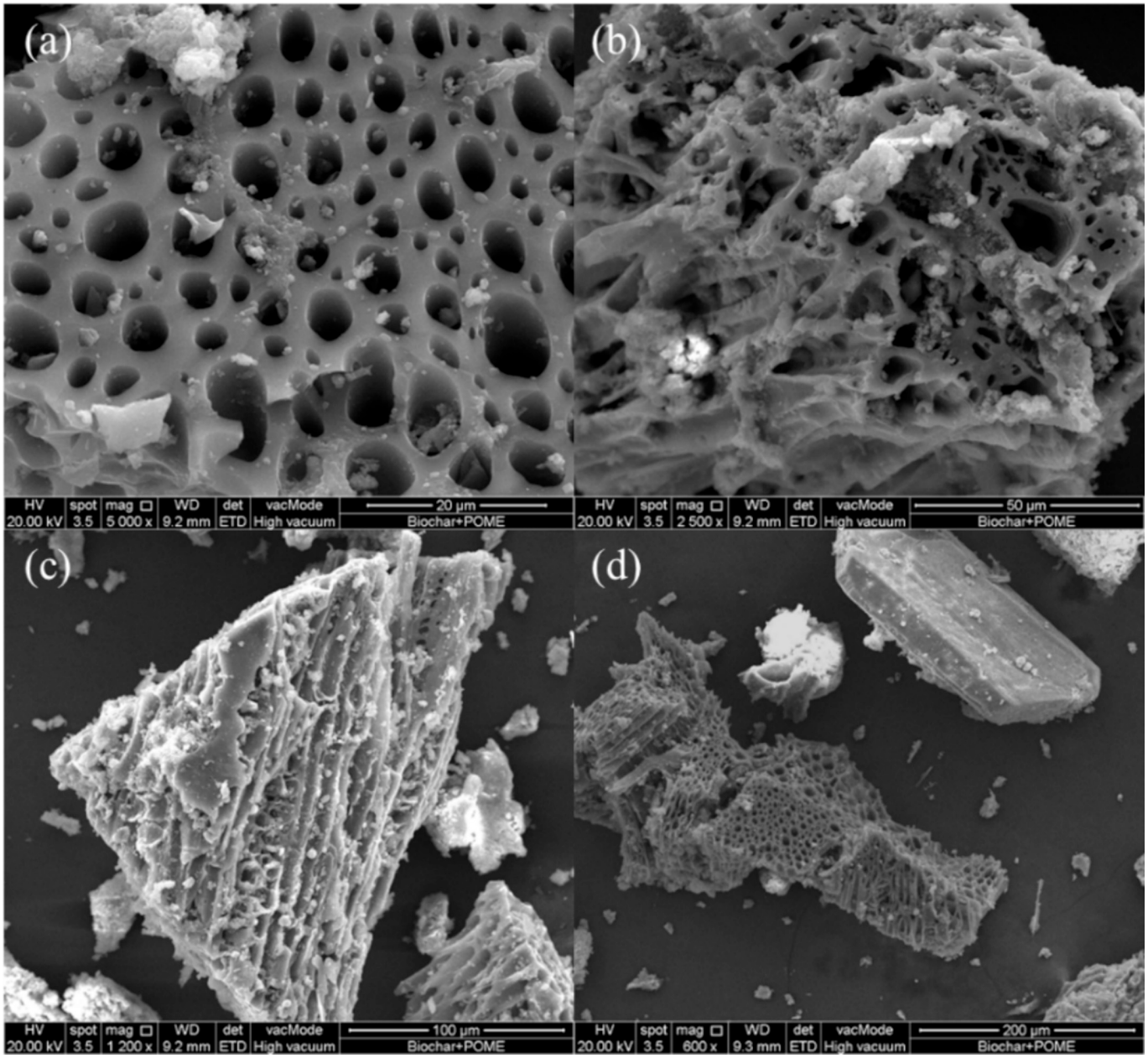

Fig. 8. SEM micrographs of biochar after AD process with a magnification of (a) 5000 times, (b) 2500 times, (c) 1200 times and (d) 600 times.

Table 4
ANOVA results for VS removal.

Source	Sum of square	Degree of Freedom	Mean square	F-value	p-value	
Model	88.08	6	14.68	1.290	0.3116	not significant
A-Biochar (g)	8.57	1	8.57	0.756	0.3966	
B-FI ratio	0.38	1	0.38	0.033	0.8575	
C-OL (g VS/L)	5.44	1	5.44	0.480	0.4977	
AB	0.04	1	0.04	0.004	0.9526	
AC	0.25	1	0.25	0.022	0.8828	
BC	27.13	1	27.13	2.390	0.1403	
Residual	192.74	17	11.34	–	–	
Cor Total	280.82	23	–	–	–	

For AD with biochar addition, the independent variable, OL (C) is shown to have the greatest impact on the biogas production. With constant biochar dosage (A) and FI ratio (B), a high OL (C) leads to more biogas production. The biochar dosage (A) and OL (C) also show impact to the biogas production by looking at Eq. 7. An optimal biochar dosage and FI ratio within the AD system are likely to lead to enhanced biogas production.

3.4.1.3. Methane yield (R3). The best fit model to describe methane yield is suggested to be the 2FI model. Table 6 listed the ANOVA results for the model. The model has an overall p-value of 0.0023 and F-value of 5.62. This implies that the model is significant, with the combination of FI ratio and OL (BC) to be the most significant model terms by having a p-value of 0.0020. The FI ratio (B) is also a weakly significant term with a p-value <0.05.

The adequate precision of 6.7848 shows that the model is tolerable.

Table 5
ANOVA results for biogas production.

Source	Sum of square	Degree of Freedom	Mean square	F-value	p-value	
Model	1.04 E+07	6	1.74 E+06	32.40	<0.0001	significant
A-Biochar (g)	2.99 E+05	1	2.99 E+05	5.56	0.0306	
B-FI ratio	36,275.12	1	36,275.12	0.68	0.4227	
C-OL (g VS/L)	4.21 E+05	1	4.21 E+05	7.83	0.0124	
AB	3713.90	1	3713.90	0.71	0.4126	
AC	12,714.97	1	12,714.97	0.24	0.6329	
BC	2.41 E+06	1	2.41 E+06	44.79	<0.0001	significant
Residual	9.13 E+05	17	53,732.60	–	–	
Cor Total	1.14 E+07	23	–	–	–	

Table 6
ANOVA results for methane yield.

Source	Sum of square	Degree of Freedom	Mean square	F-value	p-value	
Model	0.0832	6	0.0139	5.62	0.0023	significant
A-Biochar (g)	0.0002	1	0.0002	0.08	0.7814	
B-FI ratio	0.0122	1	0.0122	4.95	0.0399	significant
C-OL (g VS/L)	0.0044	1	0.0044	1.79	0.1985	
AB	0.0031	1	0.0031	1.24	0.2812	
AC	0.0030	1	0.0030	1.23	0.2829	
BC	0.0328	1	0.0328	13.31	0.0020	significant
Residual	0.0420	17	0.0025	–	–	
Cor Total	0.1252	23	–	–	–	

The R^2, adjusted R^2 and predicted R^2 are calculated to be 0.6648, 0.5465 and 0.2378, respectively. The difference between the adjust R^2 and predicted R^2 is >0.2, illustrating that there is a large block effect with the model. Therefore, model reduction should be considered. For methane yield, the regression equation and the reduced regression equation in terms of the independent variables are shown in Eq. 8 and Eq. 9, respectively.

$$\textit{Methane yield} = 0.2729 + 0.0054 \times A - 0.1480 \times B + 0.0857 \times C - 0.1150 \times AB + 0.1116 \times AC - 0.0658 \times BC \quad (8)$$

$$\textit{Methane yield} = 0.2729 - 0.1480 \times B - 0.0658 \times BC \quad (9)$$

From the reduced equation, it is shown that a reduction in FI ratio and OL yields higher methane production and the biochar dosage does not show an significant impact on the methane yield. The FI ratio is found to have the most impact on methane yield. This dependency is likely attributed to the feasibility of biodegradation of the feed (POME), which is crucial for the methane production during AD process [44].

3.4.2. *Perturbation plots*

The interactions among the three independent and three response variables can be demonstrated by using perturbation plots (Fig. 9). From the perturbation plot of the VS removal, depicted in Fig. 9(a), the steepest line corresponds to OL (C), indicating it has the greatest impact on VS removal. An inverse relationship is observed between VS removal and the OL of the feed (C). The OL (C) line exhibits the widest range along the y-axis, followed by the biochar dosage (A) and FI ratio (B)

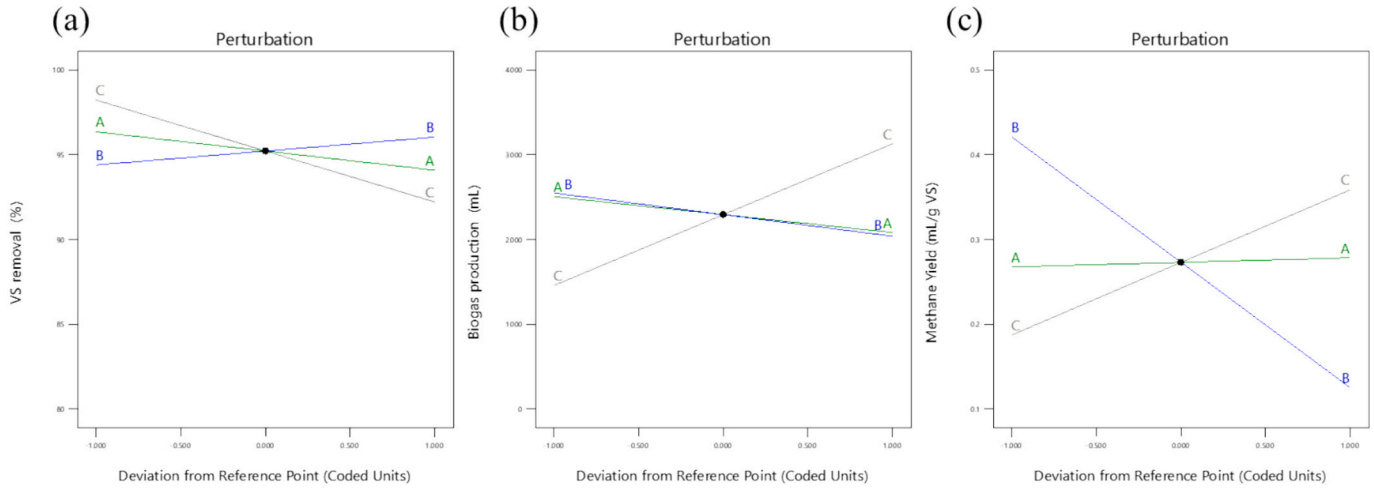

Fig. 9. Perturbation plots for (a) VS removal, (b) biogas production and (c) methane yield.

which show similar coverage. While biochar dosage shows a slightly negative effect, the FI ratio shows a slightly positive effect on the VS removal. The ranking of sensitivity for VS removal is: C > B > A.

Fig. 9(b) depicts the perturbation plot for biogas production, OL (C), has a proportional relationship with the biogas production, exhibiting the most influence on it, where an increase in OL (C) enhances the biogas production. The biochar dosage (A) and FI ratio (B) show slightly negative impact on the production of biogas. The ranking of sensitivity for biogas production is: C > B > A.

The perturbation plot of methane yield, shown in Fig. 9(c), demonstrates that the FI ratio (B) has the largest negative impact on the methane yield. The OL (C) also shows positive influence on the methane yield, but not as significant as the FI ratio (B). The biochar dosage (A) exhibits a slightly positive effect on methane yield. The ranking of sensitivity for methane yield is: B > C > A.

The differing trends observed for methane yield compared to VS removal and biogas production can be attributed to the distinct mechanisms affecting each response. While VS removal and biogas production are more directly related to the overall microbial degradation of organic matter, methane yield is more sensitive to the balance between substrate availability and the microbial processes involved in methanogenesis. In particular, the FI ratio (B) negatively influences methane yield, likely due to its effect on the metabolic pathways favoring methane production. In contrast, OL (C) has a positive but less pronounced impact on methane yield, suggesting that beyond a certain organic load, further increases in feed may not significantly enhance methane production. Biochar dosage (A) has a minor but positive effect on methane yield, which may enhance microbial activity, but the impact is weaker compared to the other responses.

3.4.3. 3D response surface

The 3D surface response plots were generated to explore the interactions among the independent variables and their impact on the response variables. Fig. 10 shows the 3D surface response plots of VS removal. The plots show VS removal efficiencies of 93–99 % upon completing the AD process, indicating effective degradation of organic solids into biogas by anaerobic microorganisms. Consequently, this process led to a reduction in residual solid content within the digestate, which has positive implications for its management and disposal, potentially enhance its value as a fertiliser or soil amendment [71].

Fig. 10(a) shows that the highest VS removal is achieved with a biochar dosage of 0 g and an FI ratio of 1.00. Nonetheless, the reliability of this finding is questionable due to the 2FI model's lack of statistical significance with low R^2 (Table A4). This indicates that the model does not accurately capture the relationship between the independent variables and VS removal, making the conclusions drawn from the surface plots unreliable. Fig. 10(b) and (c) suggest that the FI ratio has a dominant effect on VS removal at lower organic loading (OL) and that VS removal decreases at higher OL. However, these trends may not be valid for prediction due to the inadequacies of the model.

Several studies have found that the introduction of biochar to AD process of food waste shows significant effect on the removal of the feed's VS content ([72]; X. [73]). Pilli et al. [74] has suggested that the increased VS reduction results in higher methane production during AD process and further reduces the amount of stabilised organic solids in digestate for disposal. Conversely, no significant trend correlating biochar dosage and FI ratio to the VS removal was observed in this study. Addition of biochar into the AD system does not affect the efficiency of VS removal. This effective VS removal marks the good biodegradability of organic content in the POME, unaffected by the biochar dosage and FI ratio. The lack of significant terms and the minimal variability in VS removal highlight that the chosen factors may not be the main drivers for predicting VS removal. This suggests that the system operates efficiently within the selected conditions, and that other factors, such as microbial community dynamics or environmental conditions, may be more influential in determining the slight differences in VS removal.

Given the high biodegradability of POME and the system's current performance, the subsequent optimization analysis will focus on more sensitive responses, such as methane yield or biogas composition, where variations are more pronounced and statistically significant (p-values <0.05). The observed high VS removal efficiency suggests that the system may be approaching its optimal performance, thus limiting the potential for further improvements with the current factors. This result is promising for future scale-up studies, as effective biodegradation has been achieved with the chosen FI, OL, and biochar dosage ranges. Therefore, investigating alternative operational parameters or evaluating long-term stability could offer valuable insights for further enhancing system performance.

The 3D surface response plots in Fig. 11 elucidate the complex interactions between biochar dosage, FI ratio, and OL on biogas production. Fig. 11(a) demonstrates that maximum biogas production can be achieved under two distinct conditions: either with a high biochar dosage at an FI ratio of 0.2, or without biochar at an FI ratio of 1.0. The FI ratio represents the proportion of organic feed to inoculum. A high FI ratio provides more organic material relative to inoculum, potentially enhancing microbial activity and biogas production. However, if the FI ratio is too high, it may lead to imbalances or inhibit microbial efficiency.

Conversely, a low FI ratio with sufficient biochar can counterbalance this issue by offering better microbial support and substrate stability. This suggests that biochar's impact on biogas production is strongly influenced by the FI ratio. Lower FI ratios appear to benefit more from

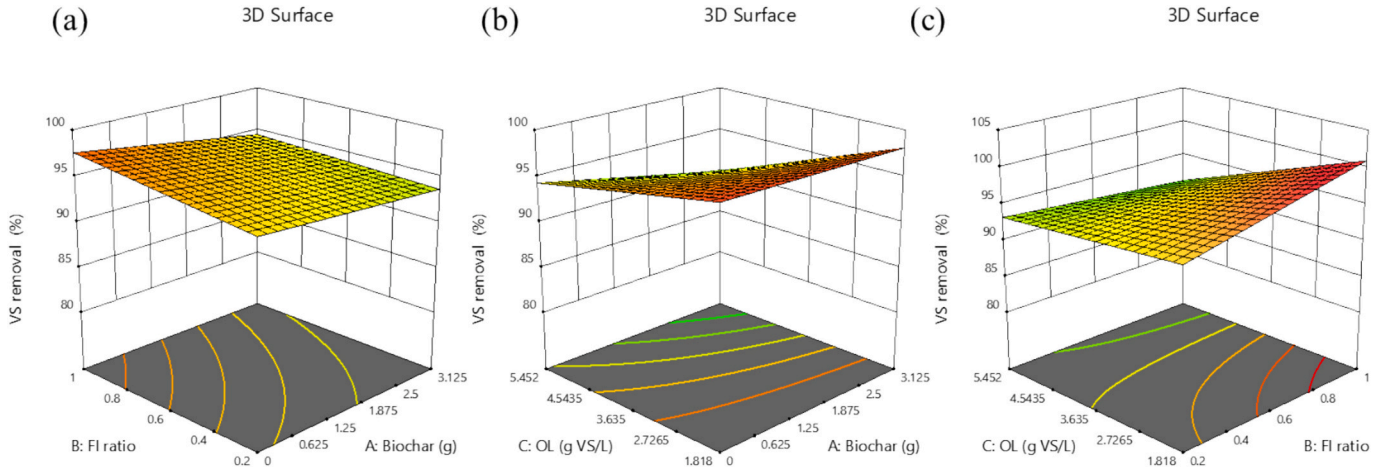

Fig. 10. Three-dimensional response surface plots of VS removal, as a function of (a) biochar dosage and FI ratio, (b) biochar dosage and OL, and (c) FI ratio and OL.

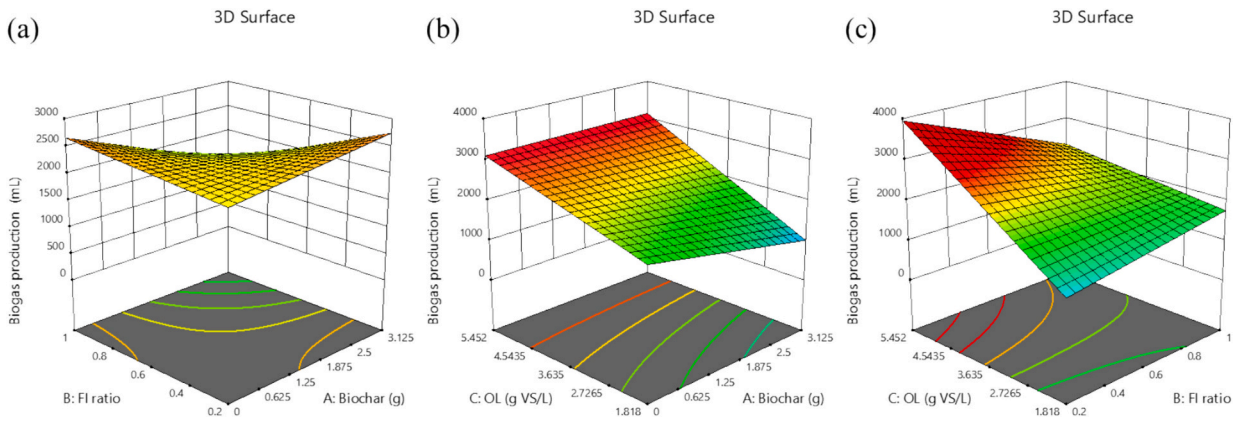

Fig. 11. Three-dimensional response surface plots of biogas production, as a function of (a) biochar dosage and FI ratio, (b) biochar dosage and OL, and (c) FI ratio and OL.

biochar addition, as it enhances microbial activity that might otherwise be limited by the reduced organic feed. At a high FI ratio (1.00) with no biochar, the system may still operate efficiently, as the higher organic load could provide sufficient nutrients and favorable conditions for microbial activity without the need for biochar.

This system's response to varying conditions highlights multiple pathways for optimizing biogas production. High biochar dosage can enhance performance at low FI ratios, while a high FI ratio might achieve similar outcomes without biochar. This indicates that either supporting microbial activity with biochar or optimizing the feed-to-inoculum ratio can lead to maximum biogas production, depending on the operational conditions.

Fig. 11(b) explores the interaction between OL and biochar dosage. At low OL, increasing the biochar dosage appears to have a negative impact on biogas production, which could be attributed to the inhibitory effects of excessive biochar that may disrupt microbial equilibrium. However, at maximum OL, biochar addition enhances biogas production, regardless of the dosage level. This suggests that at higher organic loads, biochar plays a more prominent role, potentially by improving system stability under stressed conditions or promoting microbial syntrophy, particularly in environments with elevated substrate availability. This observation points to the adaptive role of biochar, which appears to be more beneficial in high-stress scenarios where microbial communities are tasked with processing large amounts of organic material.

In Fig. 11(c), the effect of OL on biogas production is more pronounced than the effect of the FI ratio, with the highest biogas yields observed at an FI ratio of 0.2 and maximum OL. This highlights the critical role of OL as a key driver of biogas production, where increased substrate availability enhances microbial activity and increases biogas output. The FI ratio of 0.2, indicating a higher proportion of inoculum relative to the substrate, suggests that this ratio provides a microbial population density sufficient to accelerate the degradation process and optimize biogas yields at high substrate levels. While the FI ratio is influential, it primarily modulates the impact of OL rather than serving as the main determinant. These findings are consistent with the earlier ANOVA analysis (Table 6), which identified biochar dosage and OL as significant factors influencing biogas production.

The introduction of biochar into the AD process has led to considerable variability in biogas production depending on dosage. Previous studies, such as Rosi et al. [84], have documented enhanced biogas yields with biochar addition, a trend corroborated in mesophilic digestion processes involving wastewater sludge [23]. However, the current study suggests that excessive biochar can inhibit the degradation of POME, indicating the existence of an optimal dosage threshold beyond which biochar may impede rather than enhance biogas production. This finding necessitates a more refined understanding of the balance between biochar's benefits and its potential to create adverse conditions, such as inhibition of key microbial populations.

Conversely, when biochar is added in optimal quantities, it significantly enhances the rate of biogas production compared to control sets with no biochar addition. Several studies have demonstrated that an optimal amount of biochar addition can significantly enhance the methane production of AD [65,75]. For instance, Asefa et al. [76] have

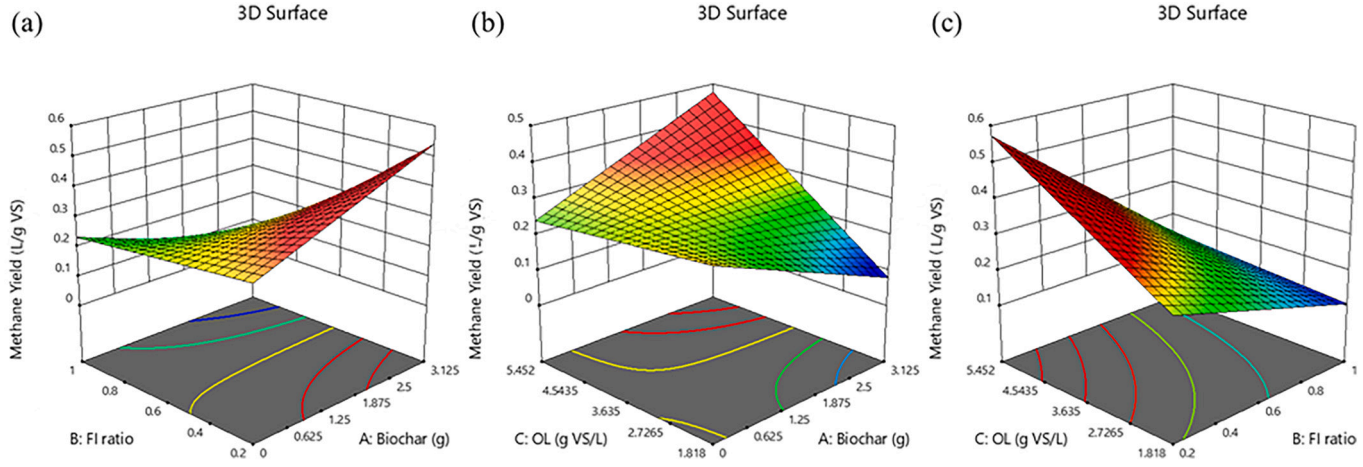

Fig. 12. Three-dimensional response surface plots of methane yield, as a function of (a) biochar dosage and FI ratio, (b) biochar dosage and OL, and (c) FI ratio and OL.

proven that 15 % of biochar addition led to a three-fold increase in methane production from the AD of tannery wastewater. This positive effect may be attributed to the presence of trace metals within biochar, which can act as micronutrient supplements for microbial communities, thereby accelerating anaerobic processes. This observation is also consistent with the findings of Cai et al. [82], who reported a more pronounced effect of smaller biochar dosages on biogas yield. The results highlight the importance of optimizing biochar dosage to harness its benefits while avoiding the inhibitory effects associated with excessive addition. Based on these results, the optimal conditions for achieving maximum biogas production are high OL, a low FI ratio, and a moderate biochar dosage.

Fig. 12 presents the 3D surface response plots for methane yield. Fig. 12(a) shows the effects of biochar addition and the FI ratio on methane yield, with biochar dosage having a stronger influence. As the biochar dosage increases, methane yield also increases. The methane yield peaks at 0.54 L /g VS when using a low FI ratio of 0.2 in conjunction with a high biochar dosage. This observation is consistent with the trend observed in Fig. 11(a), where maximum biogas production was also achieved under similar conditions of a low FI ratio and high biochar dosage. Both figures collectively indicate that a low FI ratio, combined with substantial biochar addition, facilitates the effective utilization of biochar, thereby enhancing microbial activity and resulting in increased biogas production and methane yield.

This finding agrees with the study by Cao et al. [85], which observed a decrease in methane production rate with an increasing FI ratio. A high FI ratio corresponds to a greater proportion of organic material relative to the inoculum or microbial biomass. Although a higher organic load can provide more substrate for biogas production, it may also stress the microbial community if the inoculum is insufficient. This imbalance can lead to reduced microbial efficiency and decreased conversion rates of organic matter into methane. Thus, maintaining an appropriate FI ratio is essential to ensure adequate microbial density and activity, optimizing both methane yield and overall biogas production.

From Fig. 12(b), it is evident that biochar dosage exerts a more significant influence on methane yield compared to OL. The plot shows that methane yield peaks at high OL when combined with substantial biochar dosage, indicating that elevated biochar levels enhance microbial processes and substrate utilization, particularly under high OL conditions. Interactive effect is also observed, particularly when OL is low, where increasing biochar dosage results in a reduction in methane yield. This phenomenon can be explained by several factors. At low OL, the limited availability of organic material may constrain microbial growth and activity, despite the presence of biochar. Excessive biochar in such conditions could disrupt the microbial balance or create less optimal conditions for microbial processes. Furthermore, the insufficient organic substrate might not adequately support the increased biochar dosage, thereby diminishing the overall efficiency of methane production. These findings highlight the critical importance of balancing biochar dosage with OL to achieve optimal methane yield.

Fig. 12(c) demonstrates that methane yield increases significantly with higher OL but decreases with an increasing FI ratio. Higher OL is associated with higher methane yields, which aligns with the understanding that more substrates promote microbial activity and methane generation. The maximum methane yield is achieved with a low FI ratio (indicating high inoculum concentration) and high OL, highlighting the critical role of balancing substrate availability and microbial density in the AD process.

ANOVA analysis, perturbation plots, and response surface plots collectively highlight the significant influence of the FI ratio. Based on these results, it is essential to maintain a low FI ratio, moderate biochar dosage, and high OL to maximize methane yield. This optimization will be further explored in the next section.

Table 7
Optimized and validation results for AD system performance with biochar addition.

Variables	Units	Value	Validation values	Deviation (%)
A-Biochar	g	0.500	0.5	0
B-FI ratio	–	0.266	0.27	1.48
C-OL	g VS/L	4.536	4.5	0.8
R1-VS removal	%	94.695	95.1	0.43
R2-Biogas Production	mL	2989.887	2950	1.34
R3-Methane Yield	L/g VS	0.360	0.355	1.41

3.5. Optimisation using RSM

In the optimization phase of this study, the goals for VS removal, biogas production, and methane yield were set to “maximize,” while the independent variables of OL and FI ratio were set to “in range,” and biochar dosage was set to “minimize.” This prioritization reflects the dual objectives of maximizing both energy recovery and waste reduction. The maximized biogas production and methane yield represent critical profit sources for palm oil mills, either by generating electricity or selling the biogas as a product. Additionally, achieving high VS removal efficiency significantly aids in digestate management and disposal, while contributing to enhanced biogas and methane production. As more organic solids are degraded, a greater volume is converted into biogas, thus reducing waste volume and increasing energy yields.

By using RSM in Design Expert software, the optimized values with a high desirability of 0.940 for the AD of POME with biochar addition are obtained, shown in Table 7. This suggests that the software successfully identified the optimal combination of independent and response variables to achieve the desired outcomes with a high degree of accuracy. The biochar dosage was optimized at 0.50 g, which enhances microbial activity and nutrient availability while keeping costs low. OL is optimized at 4.536 g VS/L, a level that ensures sufficient organic matter is available for microbial activity while allowing for effective degradation of the organic content in POME. The optimized FI ratio of 0.266 provides adequate amount of inoculum to support microbial growth, which leads to higher VS removal efficiency. This promotes more complete degradation of organic solids in POME, leading to a higher-quality effluent with reduced residual organic matter. This outcome highlights the critical importance of balancing the substrate-to-inoculum ratio to optimize both methane yield and the overall efficiency of the anaerobic digestion process.

Overall, the optimized response values generated from the software shows the best result for an AD system of POME with biochar addition. The solution suggests that an AD system with a low FI ratio of 0.266 and moderate OL of 4.536 g VS/L can achieve enhanced VS removal efficiency, biogas production, and methane yield with a low biochar dosage of 0.5 g. This outcome is beneficial from a cost perspective, as a lower biochar dosage still provides significant performance improvements, offering enhanced biogas production while minimizing costs associated with biochar addition.

The optimized data was validated by performing the AD under the proposed optimum conditions in triplicate. This study produced promising results, with an average VS removal of 95.1 %, biogas production of 2950 mL, and a methane yield of 0.355 L/g VS, showing low

Table 8
Parameters and statistical indicators of each kinetic model for Set 20.

Kinetic model	A (mL/g VS)	μ_m (mL/g VS/day)	λ (day)	R^2	RMSE
MGM	2.9408	0.0925	−0.3816	0.9721	0.1126
LFM	2.5526	0.0959	0.3907	0. 9618	0.1317
TFM	6.1094	0.1055	−0.3362	0.9850	0.0827

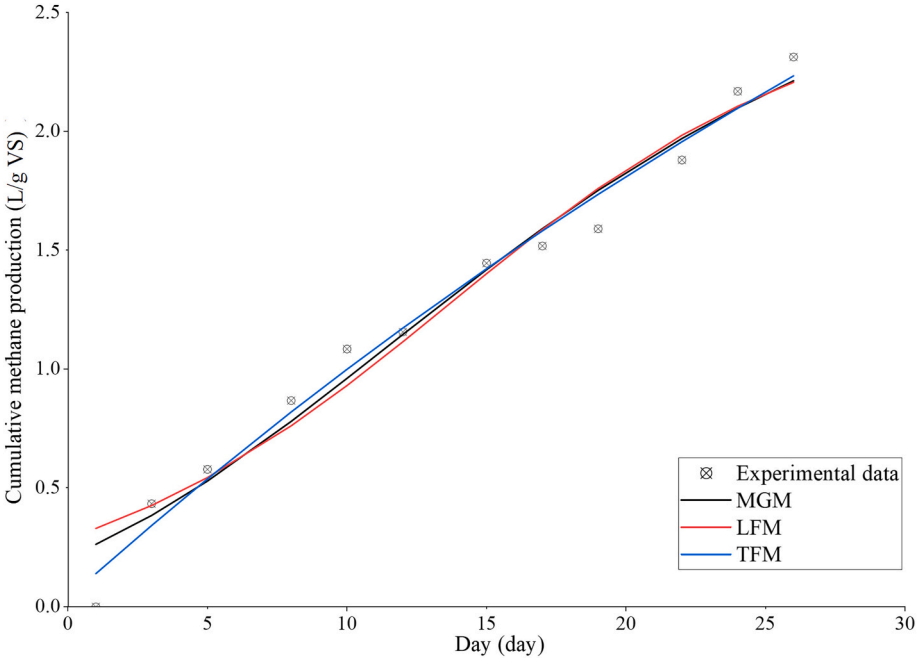

Fig. 13. Cumulative methane production of Set 20 with kinetic model curve fittings.\.

deviations of <1.4 % from the predicted values (Table 7). Notably, the methane yield achieved in this study surpasses those reported by Shi et al. [70] and Ngo et al. [21]. These findings imply the successful development of a mathematical model to predict and optimize methane yield through biochar addition with high accuracy.

3.6. Kinetic studies

A kinetic study was conducted following the optimization to further analyze the methane production behavior under the optimal conditions. Kinetic studies of cumulative methane production were performed on Set 20 with 1.0 g of biochar dosage, an FI ratio of 1.0, and an OL of 5.45 g VS/L, as it exhibited the highest methane production from the AD experiment. Table 8 lists the calculated results for the parameters, A, μ_m, and λ for each kinetic model, along with the calculated RMSE and R^2 values, which were used to validate the models mathematically.

The three modelled kinetic models including MGM, LFM and TFM are compared with the experimental data, as plotted in Fig. 13. All three models demonstrated a good fit to the cumulative methane production. Upon validation, Set 20 is found to be well-fitted in all three models, displaying high R^2 values (>0.96) and small RMSE values (<0.2). This indicates minimal errors in methane yield prediction at each data point.

The selection of TFM as the most appropriate model for this biochar addition study is based on its enhanced ability to accurately represent the methane production dynamics relative to the other models. Its R^2 and RMSE values suggest that the model provides a more accurate representation of the AD process with the addition of biochar. However, the linear characteristic of cumulative methane production in TFM contrasts with the sigmoidal curve observed in other AD studies, where models such as MFM and LFM provide better fits [77,78]. The better fit of TFM may be attributed to the biochar addition, which minimized the lag phase and enhanced the biodegradability of POME [44]. This highlights the importance of further validating the TFM model under diverse conditions and possibly integrating other models for a more comprehensive understanding of the AD process with biochar.

4. Limitations and areas of future research

This study highlights the potential of incorporating biochar into the AD treatment of POME to boost VS removal, biogas production and methane yield by both experiment and computational studies. To translate these findings into real-world applications, several key limitations must be addressed for further research.

One significant limitation is the lack of scaled-up experiments. Although this study uses specific POME and inoculum sources, the optimal biochar dosage, FI ratio, and OL for efficient AD may vary depending on feedstock characteristics. Future research should include larger-scale experiments with POME from various sources. This approach could help to determine the optimal biochar dosages required for different POME compositions and evaluate the broader applicability of this technique across various palm oil mills. Additionally, investigating lower biochar dosages (<0.5 g) could potentially reduce costs. An economic analysis should be conducted to evaluate additional expenses such as biochar cost, processing cost, and operational adjustments required at an industrial scale to support industry investment.

Moreover, this work predominantly focuses on VS removal, biogas production and methane yield. While these are the key metrics, a more comprehensive understanding of the AD performance with biochar addition requires the investigation on other parameters. The influence of feedstock and processing conditions on biochar morphology are reported, particularly its pore size, adsorption capacity and cation exchange capacity [23,29]. Further exploration is necessary on the feedstock and operating conditions for biochar production to enhance the AD for POME treatment.

Future research should aim to further elucidate the mechanisms by which biochar interacts with microbial communities under varying OL conditions. Identifying optimal biochar dosages that maximize biogas yield without compromising system stability is crucial. Additionally, examining the bacterial species present in the biochar could provide valuable insights into microbial interactions and performance. This can be achieved by extracting DNA from biochar, amplifying the 16S rRNA gene via PCR, and sequencing the resulting products to characterize the microbial community present on the biochar surface.

Furthermore, although the TFM model is chosen as the most suitable for this biochar addition study, a kinetic study should be conducted to validate the TFM model under various operational conditions and consider integrating additional models for a more comprehensive understanding of the AD process with biochar. This further study is crucial

because the TFM model, while currently effective, may not capture all complexities of the AD process across different scenarios. Incorporating additional models could reveal underlying details in microbial interactions and biochar effects that the TFM model alone may not address. By refining kinetic modeling and improving prediction accuracy, this approach will enhance our understanding of how biochar influences methane yield and overall AD performance, ultimately leading to more effective optimization strategies.

In addition, this work does not address the impact on nutrient content within the digestate. Biochar has been shown to influence the nutrient levels within the substrate. Analyzing volatile fatty acids (VFAs), total nitrogen (TN), total phosphorus (TP), and the carbon-to-nitrogen (C/N) ratio could yield valuable insights for optimizing nutrient content in the digestate. A deeper understanding of these factors is beneficial for generating a nutrient-rich digestate alongside biogas production, maximizing the resource recovery potential of POME treatment through AD.

Finally, future research should include power analysis to refine experimental design, ensuring that sample sizes and the number of experimental runs are statistically robust and sufficient to detect significant differences in outcomes. Additionally, incorporating a meta-analysis comparing biochar's effects on biogas production and methane yield across various studies would provide valuable insights into its broader impact. This approach will help identify consistent trends, address discrepancies across different experimental conditions, and enhance the overall reliability of the results. By integrating power analysis with meta-analysis, future research can optimize resource utilization and strengthen the foundation for further advancements in the AD of POME using biochar.

5. Conclusion

In this study, the effects of biochar addition on the anaerobic digestion (AD) of palm oil mill effluent (POME) were investigated. This study validated the feasibility of biochar addition as an improvement to enhance AD performance. Experiments revealed varying trends in volatile solids (VS) removal efficiency, biogas production, and methane yield with variations in feed-to-inoculum (FI) ratios, biochar dosages, and organic loading (OL). Adequate amounts of biochar addition demonstrated positive impacts across these parameters. It minimized the lag phase, boosted the conversion of VS into biogas, and ultimately improved the overall AD performance. Specifically, biogas production, methane yield, and VS removal were enhanced by 45.0 %, 73.3 %, and 98.2 %, respectively. The synergistic effects of biochar addition were evident as it enhanced the habitat provided by macropores within the biochar for microbial growth, which promoted the degradation of organic matter.

To build on these findings, Response Surface Methodology (RSM) was employed to optimize the process conditions for maximizing VS removal, biogas production, and methane yield. Central Composite Design (CCD) of RSM was used to explore the relationships between independent and response variables. To achieve optimal conditions, a combination of a low biochar dosage of 0.50 g (equivalent to 2 g/L of reactor volume), a low FI ratio of 0.266, and a high OL of 4.536 g VS/L was identified. This balance of substrate and inoculum availability with the appropriate biochar dosage resulted in a predicted biogas production of 2989.887 mL, a methane yield of 0.36 L/g VS, and a VS removal of 94.7 %. These results were validated in duplicate under the optimized conditions, confirming the model's accuracy with <1.4 % deviation from the predicted values.

Following this optimization, a kinetic study was conducted to analyze methane production behavior under the optimal conditions. The kinetic study compared the MGM, LFM, and TFM models, identifying TFM as the most suitable model for predicting methane yield due to its minimal error, low RMSE, and R^2 value closest to 1. This kinetic study confirmed that biochar significantly influences the dynamics of methane production, with synergistic effects contributing to reducing the lag phase and enhancing POME biodegradability. However, further validation of the TFM model under diverse conditions is necessary. Integrating additional kinetic models could offer a more comprehensive understanding of the AD process with biochar, refining predictions and optimizing methane yield across various scenarios.

This sequential approach which combines the optimization with kinetic analysis demonstrates a thorough evaluation of biochar's impact on AD performance. Biochar-enhanced AD provides a sustainable method for managing POME, generating valuable biogas, and potentially addressing the variability in POME characteristics and flow due to crop seasons. The optimal conditions identified can serve as a basis for scaling up to large-scale applications. For large-scale systems, it is expected that maintaining these optimal conditions will result in increased operational efficiency, improved biogas yields, and enhanced resource recovery potential, contributing to a more sustainable palm oil industry. Future work should focus on scale-up experiments with different POME sources to determine optimal biochar dosages for varied compositions. Additionally, investigating other parameters affecting nutrient content in the digestate could further enhance AD performance, broadening its applicability across palm oil mills and maximizing resource recovery potential.

CRediT authorship contribution statement

Shaet Jing Yan: Writing – original draft, Visualization, Validation, Software, Methodology, Investigation, Formal analysis, Data curation, Conceptualization. **Yi Jing Chan:** Writing – review & editing, Supervision, Resources, Project administration, Funding acquisition, Conceptualization. **Suchithra Thangalazhy-Gopakumar:** Writing – review & editing, Supervision, Resources. **Timm Joyce Tiong:** Writing – review & editing. **Jun Wei Lim:** Writing – review & editing.

Declaration of competing interest

The authors declare that they have no known competing financial interests or personal relationships that could have appeared to influence the work reported in this paper.

Acknowledgements

The author would like to acknowledge the support extended by the University of Nottingham Malaysia in facilitating this research project.

Appendix A

Table A1
Characteristics of POME in this study and the effluent discharge standard [79].

Characteristics[a]	POME in this paper	Environmental Quality Act[b]
TS	59.14	–
VS	10.91	–
BOD	34.99	0.1
COD	108.77	–
BOD/COD	0.32	–
pH	4.62	5–9

[a] Indicates that all parameters are in g/L unit except for BOD/COD and pH.
[b] Parameters limit of Environmental Quality (Prescribed Premises) for Crude Palm Oil (Amendment) Regulations 1977.

Table A2
Experiment parameters.

Set	FI ratio	Feed			OL (g VS/L)
		POME (mL)	Inoculum (mL)	Biochar (g)	
1	0.16	28	175	–	1.20
2	0.16	28	175	0.5	1.20
3	0.16	28	175	1.0	1.20
4	0.16	28	175	1.5	1.20
5	0.16	28	175	2.0	1.20
6	0.40	70	175	–	3.05
7	0.40	70	175	0.5	3.05
8	0.40	70	175	1.0	3.05
9	0.40	70	175	1.5	3.05
10	0.40	70	175	2.0	3.05
11	0.40	70	175	2.5	3.05
12	0.65	78	150	–	3.40
13	0.65	78	150	0.5	3.40
14	0.65	78	150	1.0	3.40
15	0.65	78	150	1.5	3.40
16	0.65	78	150	2.0	3.40
17	0.65	78	150	2.5	3.40
18	1.00	125	125	–	5.45
19	1.00	125	125	0.5	5.45
20	1.00	125	125	1.0	5.45
21	1.00	125	125	1.5	5.45
22	1.00	125	125	2.0	5.45
23	1.00	125	125	2.5	5.45

Table A3
Experimental results.

Set	VS removal (%)	Biogas production (mL)	Methane Yield (L/g VS)
1	93.60	550	0.1785
2	92.22	800	0.2957
3	95.97	850	0.3215
4	98.15	650	0.1879
5	96.51	500	0.1685
6	98.28	1900	0.2875
7	96.50	2150	0.3142
8	94.71	2100	0.3385
9	93.41	2100	0.3455
10	96.74	2150	0.3253
11	94.30	1900	0.2854
12	99.18	2250	0.1945
13	97.61	2300	0.2654
14	95.09	2300	0.3125
15	95.47	2550	0.2577
16	95.17	2250	0.2471
17	93.15	2150	0.2141
18	93.76	1800	0.1325
19	93.25	2450	0.1526
20	92.93	2400	0.1741
21	81.29	3000	0.1541
22	97.15	2300	0.1478

(*continued on next page*)

Table A3 (*continued*)

Set	VS removal (%)	Biogas production (mL)	Methane Yield (L/g VS)
23	91.60	1700	0.1078
Mean	94.59	1699	0.2658
Standard deviation	3.49	697	0.0883

Table A4
Fit Summary of the fitted models.

Parameters	R1: VS removal (%)	R2: Biogas Production (mL)	R3: Methane Yield (L/g VS)
Standard Deviation	3.37	231.80	0.0497
Mean	94.65	1904.19	0.2342
CV (%)	3.56	12.17	21.21
R^2	0.3136	0.9196	0.6648
Adjusted R^2	0.0714	0.8912	0.5465
Predicted R^2	−0.2021	0.8218	0.2378
Adequate Precision	3.9549	16.6072	6.7848

Data availability

Data will be made available on request.

References

[1] Statista, Palm oil consumption worldwide from 2015/2016 to 2023/2024. https://www.statista.com/statistics/274127/world-palm-oil-usage-distribution/, 2024.

[2] S.Z.Y. Foong, Y.L. Lam, V. Andiappan, D.C.Y. Foo, D.K.S. Ng, A systematic approach for the synthesis and optimization of palm oil milling processes, Ind. Eng. Chem. Res. 57 (8) (2018) 2945–2955, https://doi.org/10.1021/acs.iecr.7b04788.

[3] M.A. Bin Mohd Yusof, Y.J. Chan, C.H. Chong, C.L. Chew, Effects of operational processes and equipment in palm oil mills on characteristics of raw palm oil mill effluent (POME): A comparative study of four mills, Cleaner Waste Systems 5 (2023) 100101, https://doi.org/10.1016/j.clwas.2023.100101.

[4] H. Kamyab, S. Chelliapan, M.F.M. Din, S. Rezania, T. Khademi, A. Kumar, Palm oil mill effluent as an environmental pollutant, in: V. Waisundara (Ed.), Palm Oil, 2018, https://doi.org/10.5772/intechopen.75811. IntechOpen.

[5] J.D. Bala, J. Lalung, N. Ismail, Palm oil mill effluent (POME) treatment 'microbial communities in an anaerobic digester': a review, Int. J. Sci. Res. Publ. 4 (6) (2014) doi:https://api.semanticscholar.org/CorpusID:16862754.

[6] N.H. Zainal, N.F. Jalani, R. Mamat, A.A. Astimar, A review on the development of palm oil mill effluent (POME) final discharge polishing treatments, Journal of Oil Palm Research 29 (4) (2017) 528–540, https://doi.org/10.21894/jopr.2017.00012.

[7] Hadiyanto, M. Christwardana, D. Soetrisnanto, Phytoremediations of palm oil mill effluent (POME) by using aquatic plants and Microalge for biomass production, J. Environ. Sci. Technol. 6 (2) (2013) 79–90, https://doi.org/10.3923/jest.2013.79.90.

[8] Okereke, R.C. Ginikanwa, International journal of advanced research in biological sciences environmental impact of palm oil mill effluent and its management through biotechnological approaches, Int. J. Adv. Res. Biol. Sci 7 (7) (2020) 117–127, https://doi.org/10.22192/ijarbs.

[9] Y.Y. Choong, K.W. Chou, I. Norli, Strategies for improving biogas production of palm oil mill effluent (POME) anaerobic digestion: A critical review, Renew. Sustain. Energy Rev. 82 (2018) 2993–3006, https://doi.org/10.1016/j.rser.2017.10.036.

[10] M.S. Hybat, N.H. Abdurahman, Z.H. Yasmeen, Z. Jemaat, N.H. Azhari, Treatment of palm oil mill effluent (POME) using membrane anaerobic system (MAS), IOP Conference Series: Materials Science and Engineering 702 (1) (2019), https://doi.org/10.1088/1757-899X/702/1/012029.

[11] S.K. Al-Amshawee, M.Y.M. Yunus, A review on possible approaches of anaerobic biological processes for palm oil mill effluent: process, quality, advantages, and limitations, IOP Conference Series: Materials Science and Engineering 702 (1) (2019) 012058, https://doi.org/10.1088/1757-899X/702/1/012058.

[12] J.N. Meegoda, B. Li, K. Patel, L.B. Wang, A review of the processes, parameters, and optimization of anaerobic digestion, Int. J. Environ. Res. Public Health 15 (10) (2018) doi:10.3390%2Fijerph15102224.

[13] Y. Li, S.Y. Park, J. Zhu, Solid-state anaerobic digestion for methane production from organic waste, Renew. Sustain. Energy Rev. 15 (1) (2011) 821–826, https://doi.org/10.1016/j.rser.2010.07.042.

[14] X. Ge, L. Yang, J.P. Sheets, Z. Yu, Y. Li, Biological conversion of methane to liquid fuels: status and opportunities, Biotechnol. Adv. 32 (8) (2014) 1460–1475, https://doi.org/10.1016/j.biotechadv.2014.09.004.

[15] M.A.A. Bakar, W.J. Yahya, Z. Mohamad, Pollution reduction Technology in Palm oil Mill through effluent treatment and management, in: Journal of Advanced Vehicle System, 2016. ISSN (Vol. 1, issue 1).

[16] K.W. Kan, Y.J. Chan, T.J. Tiong, J.W. Lim, Maximizing biogas yield from palm oil mill effluent (POME) through advanced simulation and optimisation techniques on an industrial scale, Chem. Eng. Sci. 285 (2024) 119644, https://doi.org/10.1016/j.ces.2023.119644.

[17] A.J. Ward, P.J. Hobbs, P.J. Holliman, D.L. Jones, Optimisation of the anaerobic digestion of agricultural resources, Bioresour. Technol. 99 (17) (2008) 7928–7940, https://doi.org/10.1016/j.biortech.2008.02.044.

[18] M. Manga, C. Aragón-Briceño, P. Boutikos, S. Semiyaga, O. Olabinjo, C. C. Muoghalu, Biochar and its potential application for the improvement of the anaerobic digestion process: A critical review, Energies 16 (10) (2023) 4051, https://doi.org/10.3390/en16104051.

[19] C.C. Muoghalu, P.A. Owusu, S. Lebu, A. Nakagiri, S. Semiyaga, O.T. Iorhemen, M. Manga, Biochar as a novel technology for treatment of onsite domestic wastewater: A critical review, Front. Environ. Sci. 11 (2023), https://doi.org/10.3389/fenvs.2023.1095920.

[20] F. Codignole Luz, S. Cordiner, A. Manni, V. Mulone, V. Rocco, Biochar characteristics and early applications in anaerobic digestion-a review, J. Environ. Chem. Eng. 6 (2) (2018) 2892–2909, https://doi.org/10.1016/j.jece.2018.04.015.

[21] T. Ngo, L.S. Khudur, S. Hassan, K. Jansriphibul, A.S. Ball, Enhancing microbial viability with biochar for increased methane production during the anaerobic digestion of chicken manure, Fuel 368 (2024) 131603, https://doi.org/10.1016/j.fuel.2024.131603.

[22] Y. Qin, X. Yin, X. Xu, X. Yan, F. Bi, W. Wu, Specific surface area and electron donating capacity determine biochar's role in methane production during anaerobic digestion, Bioresour. Technol. 303 (2020) 122919, https://doi.org/10.1016/j.biortech.2020.122919.

[23] M. Chiappero, F. Berruti, O. Mašek, S. Fiore, Analysis of the influence of activated biochar properties on methane production from anaerobic digestion of waste activated sludge, Biomass Bioenergy 150 (2021) 106129, https://doi.org/10.1016/j.biombioe.2021.106129.

[24] M. Zhang, J. Li, Y. Wang, C. Yang, Impacts of different biochar types on the anaerobic digestion of sewage sludge, RSC Adv. 9 (72) (2019) 42375–42386, https://doi.org/10.1039/C9RA08700A.

[25] S. Chaikitkaew, P. Kongjan, O-Thong, S., Biogas production from biomass residues of palm oil mill by solid state anaerobic digestion, Energy Procedia 79 (2015) 838–844, https://doi.org/10.1016/j.egypro.2015.11.575.

[26] L. Levén, A.R.B. Eriksson, A. Schnürer, Effect of process temperature on bacterial and archaeal communities in two methanogenic bioreactors treating organic household waste, FEMS Microbiol. Ecol. 59 (3) (2007) 683–693, https://doi.org/10.1111/j.1574-6941.2006.00263.x.

[27] Z. Yang, W. Wang, Y. He, R. Zhang, G. Liu, Effect of ammonia on methane production, methanogenesis pathway, microbial community and reactor performance under mesophilic and thermophilic conditions, Renew. Energy 125 (2018) 915–925, https://doi.org/10.1016/j.renene.2018.03.032.

[28] D. Johnravindar, R.D. Patria, J.T.E. Lee, L. Zhang, Y.W. Tong, C.-H. Wang, Y.S. Ok, G. Kaur, Syntrophic interactions in anaerobic digestion: how biochar properties affect them? Sustainable Environment 7 (1) (2021) https://doi.org/10.1080/27658511.2021.1945282.

[29] H. Liang, L. Chen, G. Liu, H. Zheng, Surface morphology properties of biochars produced from different feedstocks, 2016, https://doi.org/10.2991/iccte-16.2016.210.

[30] L.A. Sarabia, M.C. Ortiz, Response surface methodology, in: Comprehensive Chemometrics, Elsevier, 2009, pp. 345–390, https://doi.org/10.1016/B978-044452701-1.00083-1.

[31] S. Beg, Z. Rahman, Central composite designs and their applications in pharmaceutical product development, in: Design of Experiments for Pharmaceutical Product Development, Springer Singapore, 2021, pp. 63–76, https://doi.org/10.1007/978-981-33-4717-5_6.

[32] W.M. Marget, M.D. Morris, Central composite experimental designs for multiple responses with different models, Technometrics 61 (4) (2019) 524–532, https://doi.org/10.1080/00401706.2018.1549102.
[33] R. Uma Rani, S. Adish Kumar, S. Kaliappan, I.-T. Yeom, J. Rajesh Banu, Enhancing the anaerobic digestion potential of dairy waste activated sludge by two step sono-alkalization pretreatment, Ultrason. Sonochem. 21 (3) (2014) 1065–1074, https://doi.org/10.1016/j.ultsonch.2013.11.007.
[34] J.S.M. Tiong, Y.J. Chan, J.W. Lim, M. Mohamad, C.-D. Ho, A.U. Rahmah, W. Kiatkittipong, W. Sriseubsai, I. Kumakiri, Simulation and optimization of anaerobic co-digestion of food waste with palm oil mill effluent for biogas production, Sustainability 13 (24) (2021) 13665, https://doi.org/10.3390/su132413665.
[35] G.T.X. Yong, Y.J. Chan, P.L. Lau, B. Ethiraj, A.A. Ghfar, A.A.A. Mohammed, M. K. Shahid, J.W. Lim, Optimization of the performances of palm oil mill effluent (POME)-based biogas plants using comparative analysis and response surface methodology, Processes 11 (6) (2023) 1603, https://doi.org/10.3390/pr11061603.
[36] G. Antonopoulou, H.N. Gavala, I.V. Skiadas, G. Lyberatos, ADM1-based modeling of methane production from acidified sweet sorghum extract in a two stage process, Bioresour. Technol. 106 (2012) 10–19, https://doi.org/10.1016/j.biortech.2011.11.088.
[37] X. Chen, Z. Chen, X. Wang, C. Huo, Z. Hu, B. Xiao, M. Hu, Application of ADM1 for modeling of biogas production from anaerobic digestion of Hydrilla verticillata, Bioresour. Technol. 211 (2016) 101–107, https://doi.org/10.1016/j.biortech.2016.03.002.
[38] D.J. Batstone, D. Puyol, X. Flores-Alsina, J. Rodríguez, Mathematical modelling of anaerobic digestion processes: applications and future needs, Rev. Environ. Sci. Biotechnol. 14 (4) (2015) 595–613, https://doi.org/10.1007/s11157-015-9376-4.
[39] B. Deepanraj, V. Sivasubramanian, S. Jayaraj, Effect of substrate pretreatment on biogas production through anaerobic digestion of food waste, Int. J. Hydrogen Energy 42 (42) (2017) 26522–26528, https://doi.org/10.1016/j.ijhydene.2017.06.178.
[40] A.N. Matheri, M. Belaid, T. Seodigeng, C.J. Ngila, Modelling the kinetic of biogas production from co-digestion of pig waste and grass clippings, in: 24th World Congress on Engineering (WCE 2016), 2016.
[41] A. Donoso-Bravo, S.I. Pérez-Elvira, F. Fdz-Polanco, Application of simplified models for anaerobic biodegradability tests. Evaluation of pre-treatment processes, Chem. Eng. J. 160 (2) (2010) 607–614, https://doi.org/10.1016/j.cej.2010.03.082.
[42] D. Christie, S.P. Neill, Measuring and observing the ocean renewable energy resource, Comprehensive Renewable Energy 1-9 (1–8) (2022) 149–175, https://doi.org/10.1016/B978-0-12-819727-1.00083-2. Second Edition.
[43] D. Figueiredo, Júnior Silva, E. Rocha, What is R2 all about? Leviathan-Cadernos de Pesquisa Polútica 3 (2011) 60–68, https://doi.org/10.11606/issn.2237-4485.lev.2011.132282.
[44] Y.F. Lim, Y.J. Chan, F.S. Hue, S.C. Ng, H. Hashma, Anaerobic co-digestion of palm oil mill effluent (POME) with decanter cake (DC): effect of mixing ratio and kinetic study, Bioresource Technology Reports 15 (2021), https://doi.org/10.1016/j.biteb.2021.100736.
[45] Y.F. Lim, Y.J. Chan, F.S. Hue, S.C. Ng, H. Hashma, Anaerobic co-digestion of palm oil mill effluent (POME) with decanter cake (DC): effect of mixing ratio and kinetic study, Bioresource Technology Reports 15 (2021) 100736, https://doi.org/10.1016/j.biteb.2021.100736.
[46] P. Prasertsan, C. Leamdum, S. Chantong, C. Mamimin, P. Kongjan, O-Thong, S., Enhanced biogas production by co-digestion of crude glycerol and ethanol with palm oil mill effluent and microbial community analysis, Biomass Bioenergy 148 (2021), https://doi.org/10.1016/j.biombioe.2021.106037.
[47] T. Hai, P. Mishra, J. Mohamad Zain, K. Saini, N. Manoj Kumar, Z. Ab Wahid, Co-digestion of domestic kitchen food waste and palm oil mill effluent for biohydrogen production, Sustain Energy Technol Assess 55 (2023), https://doi.org/10.1016/j.seta.2022.102965.
[48] N.H. Zainal, N.F. Jalani, R. Mamat, A.A. Astimar, A review on the development of palm OIl mill effluent (POME) final discharge polishing treatment, Journal of Oil Palm Research 29 (4) (2018) 528–540, https://doi.org/10.21894/jopr.2017.00012.
[49] C.C. Yap, A.D.A. Bin Abu Sofian, Y.J. Chan, S.K. Loh, M.F. Chong, L.K. Lim, High organic loading rate treatment of palm oil mill effluent using a pilot-scale integrated anaerobic-aerobic bioreactor: A comprehensive performance study, Fuel 382 (2025) 133727, https://doi.org/10.1016/j.fuel.2024.133727.
[50] G.T.X. Yong, Y.J. Chan, P.L. Lau, B. Ethiraj, A.A. Ghfar, A.A.A. Mohammed, M. K. Shahid, J.W. Lim, Optimization of the performances of palm oil mill effluent (POME)-based biogas plants using comparative analysis and response surface methodology, Processes 11 (6) (2023), https://doi.org/10.3390/pr11061603.
[51] H. Farraji, N.Q. Zaman, H. Abdul Aziz, M.A. Ashraf, A. Mojiri, P. Mohajeri, Enhancing BOD/COD ratio of POME treatment in SBR system, Appl. Mech. Mater. 802 (2015) 437–442, https://doi.org/10.4028/www.scientific.net/AMM.802.437.
[52] D.J.S. Chong, Y.J. Chan, S.K. Arumugasamy, S.K. Yazdi, J.W. Lim, Optimisation and performance evaluation of response surface methodology (RSM), artificial neural network (ANN) and adaptive neuro-fuzzy inference system (ANFIS) in the prediction of biogas production from palm oil mill effluent (POME), Energy 266 (2023) 126449, https://doi.org/10.1016/j.energy.2022.126449.
[53] B. Trisakti, R. Sidabutar, Irvan, L. Adriani, J.F. Manurung, D.K. Simbolon, V. Alexander, Mohd.S. Takriff, H. Daimon, Effect of hydraulic retention time and effluent recycle ratio on biogas production from POME using UASB-HCPB fermentor assisted with ultrafiltration membrane at mesophilic condition, South African Journal of Chemical Engineering 50 (2024) 209–222, https://doi.org/10.1016/j.sajce.2024.08.012.
[54] C. Sawatdeenarunat, C. Wangnai, W. Songkasiri, P. Panichnumsin, K. Saritpongteeraka, P. Boonsawang, S.K. Khanal, S. Chaiprapat, Biogas production from industrial effluents, in: Biofuels: Alternative Feedstocks and Conversion Processes for the Production of Liquid and Gaseous Biofuels, Elsevier, 2019, pp. 779–816, https://doi.org/10.1016/B978-0-12-816856-1.00032-4.
[55] A.A. Ramón Vanegas, J. Vásquez, F. Molina, M. Peñuela Vásquez, Evaluation of anaerobic digestion of palm oil mill effluent (POME) using different sludges as inoculum, Water Resources and Industry 31 (2024) 100247, https://doi.org/10.1016/j.wri.2024.100247.
[56] Z. Tan, C.S.K. Lin, X. Ji, T.J. Rainey, Returning biochar to fields: A review, Appl. Soil Ecol. 116 (2017) 1–11, https://doi.org/10.1016/j.apsoil.2017.03.017.
[57] W. Zhao, H. Yang, S. He, Q. Zhao, L. Wei, A review of biochar in anaerobic digestion to improve biogas production: Performances, mechanisms and economic assessments, in: Bioresource Technology vol. 341, Elsevier Ltd., 2021, https://doi.org/10.1016/j.biortech.2021.125797.
[58] A. Shaaban, S.-M. Se, M.F. Dimin, J.M. Juoi, M.H. Mohd Husin, N.M.M. Mitan, Influence of heating temperature and holding time on biochars derived from rubber wood sawdust via slow pyrolysis, J. Anal. Appl. Pyrolysis 107 (2014) 31–39, https://doi.org/10.1016/j.jaap.2014.01.021.
[59] H.-J. Yang, Z.-M. Yang, X.-H. Xu, R.-B. Guo, Increasing the methane production rate of hydrogenotrophic methanogens using biochar as a biocarrier, Bioresour. Technol. 302 (2020) 122829, https://doi.org/10.1016/j.biortech.2020.122829.
[60] J. Yang, J. Zhang, J. Zhang, J. Zhang, Y. Yang, L. Zang, Roles of calcium-containing alkali materials on dark fermentation and anaerobic digestion: A systematic review, Int. J. Hydrogen Energy 46 (78) (2021) 38645–38662, https://doi.org/10.1016/j.ijhydene.2021.09.129.
[61] D. Botheju, Oxygen effects in anaerobic digestion – A review, The Open Waste Management Journal 4 (1) (2011) 1–19, https://doi.org/10.2174/1876400201104010001.
[62] Y. Chen, J.J. Cheng, K.S. Creamer, Inhibition of anaerobic digestion process: A review, Bioresour. Technol. 99 (10) (2008) 4044–4064, https://doi.org/10.1016/j.biortech.2007.01.057.
[63] J. Li, W. Shi, C. Jiang, L. Bai, T. Wang, J. Yu, W. Ruan, Evaluation of potassium as promoter on anaerobic digestion of saline organic wastewater, Bioresour. Technol. 266 (2018) 68–74, https://doi.org/10.1016/j.biortech.2018.06.066.
[64] J.-H. Ahn, T.H. Do, S.D. Kim, S. Hwang, The effect of calcium on the anaerobic digestion treating swine wastewater, Biochem. Eng. J. 30 (1) (2006) 33–38, https://doi.org/10.1016/j.bej.2006.01.014.
[65] C. Luo, F. Lü, L. Shao, P. He, Application of eco-compatible biochar in anaerobic digestion to relieve acid stress and promote the selective colonization of functional microbes, Water Res. 68 (2015) 710–718, https://doi.org/10.1016/j.watres.2014.10.052.
[66] M.-J. Kim, S.-H. Kim, Conditions of lag-phase reduction during anaerobic digestion of protein for high-efficiency biogas production, Biomass Bioenergy 143 (2020) 105813, https://doi.org/10.1016/j.biombioe.2020.105813.
[67] L. Micoli, G.D.R. Simeone, M. Turco, G. Toscano, M.A. Rao, Biochar enhances anaerobic digestion of olive mill wastewater, Chem. Eng. Trans. 99 (2023), https://doi.org/10.3303/CET2399015.
[68] N.M.S. Sunyoto, M. Zhu, Z. Zhang, D. Zhang, Effect of biochar addition on hydrogen and methane production in two-phase anaerobic digestion of aqueous carbohydrates food waste, Bioresour. Technol. 219 (2016) 29–36, https://doi.org/10.1016/j.biortech.2016.07.089.
[69] C. Wang, Y. Liu, X. Gao, H. Chen, X. Xu, L. Zhu, Role of biochar in the granulation of anaerobic sludge and improvement of electron transfer characteristics, Bioresour. Technol. 268 (2018) 28–35, https://doi.org/10.1016/j.biortech.2018.07.116.
[70] Y. Shi, M. Liu, J. Li, Y. Yao, J. Tang, Q. Niu, The dosage-effect of biochar on anaerobic digestion under the suppression of oily sludge: performance variation, microbial community succession and potential detoxification mechanisms, J. Hazard. Mater. 421 (2022) 126819, https://doi.org/10.1016/j.jhazmat.2021.126819.
[71] A. Slepetiene, J. Volungevicius, L. Jurgutis, I. Liaudanskiene, K. Amaleviciute-Volunge, J. Slepetys, J. Ceseviciene, The potential of digestate as a biofertilizer in eroded soils of Lithuania, Waste Manag. 102 (2020) 441–451, https://doi.org/10.1016/j.wasman.2019.11.008.
[72] J. Hu, K. Stenchly, W. Gwenzi, M. Wachendorf, K. Kaetzl, Critical evaluation of biochar effects on methane production and process stability in anaerobic digestion, Frontiers in Energy Research 11 (2023), https://doi.org/10.3389/fenrg.2023.1205818.
[73] X. Li, N. Shimizu, Biochar-promoted methane production and mitigation of acidification during thermophilic anaerobic co-digestion of food waste with crude glycerol: comparison with re-inoculation, Sustainable Environment Research 33 (1) (2023) 4, https://doi.org/10.1186/s42834-023-00167-w.
[74] S. Pilli, P. Bhunia, S. Yan, R.J. LeBlanc, R.D. Tyagi, R.Y. Surampalli, Ultrasonic pretreatment of sludge: A review, Ultrason. Sonochem. 18 (1) (2011) 1–18, https://doi.org/10.1016/j.ultsonch.2010.02.014.
[75] Y. Cui, F. Mao, J. Zhang, Y. He, Y.W. Tong, Y. Peng, Biochar enhanced high-solid mesophilic anaerobic digestion of food waste: cell viability and methanogenic pathways, Chemosphere 272 (2021) 129863, https://doi.org/10.1016/j.chemosphere.2021.129863.
[76] S.K. Asefa, V.R. Ancha, N.G. Habtu, L.S. Sundar, Experimental evaluation on the effect of biochar addition with anaerobic digestion of the tannery wastewater to improve biogas production, Water Reuse 13 (3) (2023) 459–474, https://doi.org/10.2166/wrd.2023.061.

[77] S. Panigrahi, H.B. Sharma, B.K. Dubey, Anaerobic co-digestion of food waste with pretreated yard waste: A comparative study of methane production, kinetic modeling and energy balance, J. Clean. Prod. 243 (2020) 118480, https://doi.org/10.1016/j.jclepro.2019.118480.
[78] C. Zhao, H. Yan, Y. Liu, Y. Huang, R. Zhang, C. Chen, G. Liu, Bio-energy conversion performance, biodegradability, and kinetic analysis of different fruit residues during discontinuous anaerobic digestion, Waste Manag. 52 (2016) 295–301, https://doi.org/10.1016/j.wasman.2016.03.028.
[79] N.S.A. Shahrifun, Characterization of palm oil mill secondary effluent (POMSE), KSCE J. Civ. Eng. 27 (2015) 144–151.
[80] Y.J. Chan, H.W. Lee, A. Selvarajoo, Comparative study of the synergistic effect of decanter cake (DC) and empty fruit bunch (EFB) as the co-substrates in the anaerobic co-digestion (ACD) of palm oil mill effluent (POME), Environ. Chall. 5 (2021) 100257.
[81] E. Sánchez, C. Herrmann, W. Maja, R. Borja, Effect of organic loading rate on the anaerobic digestion of swine waste with biochar addition, Environ. Sci. Pollut. R. 28 (29) (2021) 38455–38465, https://doi.org/10.1007/s11356-021-13428-1.
[82] J. Cai, P. He, Y. Wang, L. Shao, F. Lü, Effects and optimization of the use of biochar in anaerobic digestion of food wastes, Waste Manag. Res. 34 (5) (2016) 409–416, https://doi.org/10.1177/0734242X16634196.
[83] S. Wang, et al., Effects of rice straw biochar on methanogenic bacteria and metabolic function in anaerobic digestion, Sci. Rep. 12 (1) (2022) 6971, https://doi.org/10.1038/s41598-022-10682-2. Available at: https://doi.org/10.1038/s41598-022-10682-2.
[84] L. Rosi, et al., Enhancing biogas production in anaerobic digestion by the addition of oxidized and non-oxidized biochars, Biomass Convers. Biorefin. 14 (4) (2024) 5457–5468. Available at: https://doi.org/10.1007/s13399-022-02813-6.
[85] L. Cao, et al., Effects of temperature and inoculation ratio on methane production and nutrient solubility of swine manure anaerobic digestion, Bioresour. Technol. 299 (2020) 122552. Available at: https://doi.org/10.1016/j.biortech.2019.122552.
[86] M.A.B.M. Yusof, Y.J. Chan, C.H. Chong, C.L. Chew, Effects of operational processes and equipment in palm oil mills on characteristics of raw Palm Oil Mill Effluent (POME): A comparative study of four mills, Clean. Waste Syst. 5 (2023) 100101.
[87] M.R. Zakaria, M.A.A. Farid, Y. Andou, I. Ramli, M.A. Hassan, Production of biochar and activated carbon from oil palm biomass: current status, prospects, and challenges, Ind. Crop. Prod. 199 (2023) 116767. Available at: https://doi.org/10.1016/j.indcrop.2023.116767.
[88] Siyao Pei, Xiaodan Fan, Chunsheng Qiu, Nannan Liu, Fei Li, Jiakang Li, Li Qi, Shaopo Wang, Effect of biochar addition on the anaerobic digestion of food waste: microbial community structure and methanogenic pathways, Water Sci. Technol. 90 (3) (1 August 2024) 894–907, https://doi.org/10.2166/wst.2024.199.